Cookham Abbey: Skeletal analysis of inhumations from the 2024 and 2025 field seasons

Ceri Falys, University of Reading, Thames Valley Archaeological Services

1. Introduction

During the third and fourth field seasons of the University of Reading's excavations at Cookham Abbey (COP) (2024 and 2025), a total of 40 articulated skeletons were recovered from within Trench 2 (2024 n=26, 2025 n=14). This report details the initial results for the 2024 and 2025 individuals, providing information on the preservation of the remains, minimum number of individuals within each burial, their biological sex, age-at-death, and skeletal and dental pathology. The overall results are then combined and compared with the demographic and pathological results from 2022-23 (Figure 1a, white line = eastern end; purple line = western end). The final summary provides recommendations for the next stages of analysis to explore the lives and deaths of the people of Cookham Abbey.

1.1 Aims of the 2024-5 excavations

The 2024 excavations had three main goals:

1) To further investigate the western burials by extending the 2023 north-south sondage (originally 1.5m wide) several metres towards the east. Due to the presence of large quantities of disarticulated bone in the upper layers of soil during 2023 excavations, the soil in this area was removed in thin spits (approximately 5cm thick) to allow for the assessment of quantity of bone and possible patterns of re-deposited human remains. These were fully recorded in situ and removed to assess the presence of underlying articulated burials (see orange outline in Figure 1b).
2) Complete the excavation of burials SK2202, SK2203 and SK2204, located at the southern end of the 2023 western sondage, whose crania were discovered during 2023 (see yellow outline in Figure 1b).
3) Complete the excavation of the western row of individual graves, including the two individuals discovered at the end of 2023 (i.e., SK2217 and SK2218, see the red 'X' in Figure 1b), and explore the presence of further graves to the west of this row (see red outline in Figure 1b).

The 2025 season had three main goals:

1) To complete the excavation of two individuals that were identified at the end of 2024: SK2520 and SK2521, who were located beneath SK2500 (see blue 'X' in Figure 1c).
2) To excavate the north-west quadrant of Trench 2, reducing the area in spits to identify, record and remove any deposits of disarticulated human bone before exploring the presence of articulated burials (see green outline in Figure 1c).
3) To reduce the levels of the central portion of Trench 2 and excavate any burials encountered, in order to assess whether the well-organized rows of graves continued towards the western end of Trench 2 (see blue outline in Figure 1c).

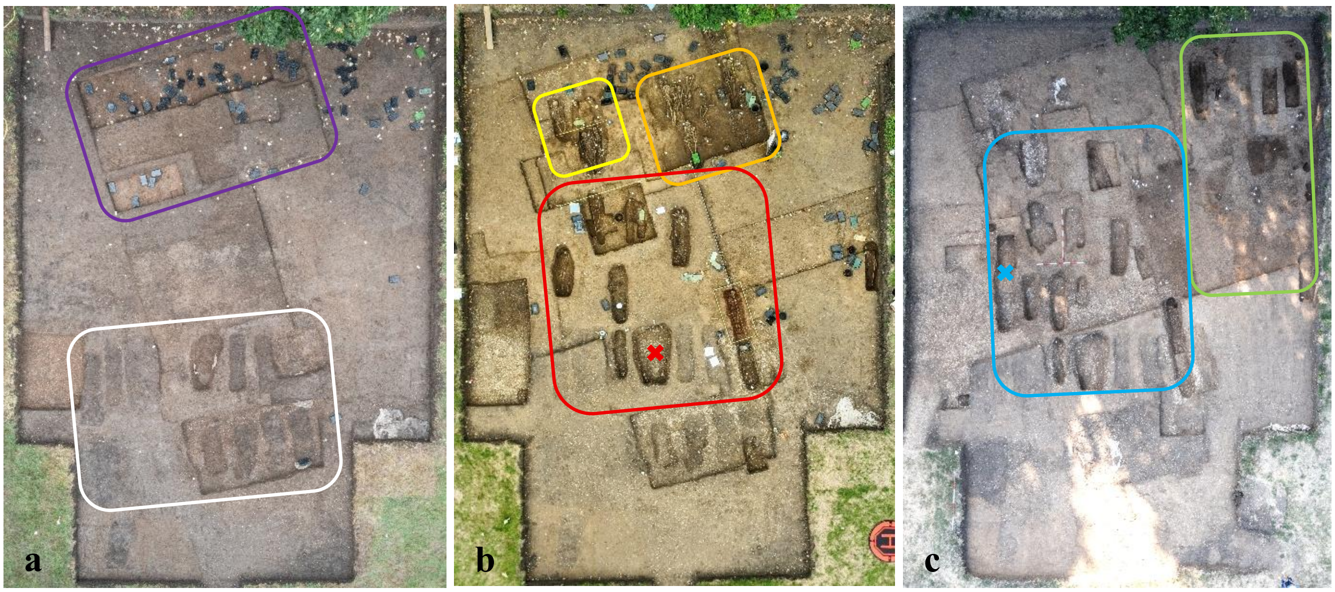

Figure 1. Progression of excavation of Trench 2. End of the field seasons 2023 (a), 2024 (b) and 2025 (c).

2. Disarticulated human remains

In total, 40 partial or complete articulated individuals were excavated during 2024 and 2025. Larger quantities of disarticulated human bone were collected from the grave fills of several burials during 2024 compared to the 2022, 2023 and 2025 excavations. There were different methods of including disarticulated remains with the new burial (Figure 2). For example, SK2500 was surrounded by randomly placed skeletal remains (Figure 2a), but during the internment of SK2504 it appears as though an attempt had been made to re-arranged the disturbed remains around the body (in approximate anatomical position), with the cranium placed above the skull of SK2504, and arms along the sides of the upper body (Figure 2b). A significant quantity of disarticulated bone was placed around the lower legs and feet of SK2502, with long bones lining the end of the grave cut and the inclusion of at least three crania.

Figure 2. Disturbed and disarticulated human bone in graves of SK2500 (a), SK2504 (b) and SK2502 (c).

In addition to the disturbed bones within the graves, deposits of disarticulated long bones and crania have been found in two (possibly three) other locations across the site, which had been arranged, perhaps, a symbolic way. The first of these “crania and crossed bones” arrangements was observed in 2023 to the north of the “long bone line” (SF1080, an approx. E-W aligned line of long bones that extended across the 1.5m width of the sondage), in which two femora had been symmetrically crossed and two crania placed in opposite quadrants (Figure 3a). The second deposit discovered in 2025, comprised a cranium placed on top of crossed bones of the upper limb and ilium and between the burials of SK2501, SK2508, and SK2526 (Figure 3b).

Figure 3. Deposits of “crania and crossed bones” discovered during 2023 (a, SF954) and 2025 (b, 1676).

3. <u>Osteological Analysis</u>

Osteological analysis of the 2024-5 burials was undertaken following guidelines by Buikstra and Ubelaker (1994), and BABAO and CIfA (Brickley and McKinley 2004, Mitchell and Brickley 2017). A summary of the findings and additional photographs for each individual can be found in Table 1, and the Skeleton Catalogue (Appendix 3).

3.1 Methods

<u>3.1.1 Surface preservation and completeness</u>

Skeletal preservation depends on several factors, both intrinsic and extrinsic to the skeleton itself. Intrinsic factors such as age, biological sex, and the overall size, shape and robusticity of the bone affect the degree of preservation. Extrinsic factors in the burial environment, post-depositional disturbance and post-excavation treatment can also affect the condition of bone. During analysis, preservation was assessed in three ways. Firstly, using a generalized grading system of three categories: poor, fair and good:

- **Poor**: all bone is highly fragmented. Most elements of the skeleton are not present or display severe damage. Trabecular bone has largely not survived, making most osteological analyses impossible.
- **Fair**: bones are moderately fragmented most commonly within the axial skeleton (i.e., skull, spine, pelvis, ribs), hindering some osteological and pathological analysis.

- **Good**: the bones have a low degree of fragmentation and the cortical bone has little or no damage with large areas of well-preserved bone, sufficient for osteological and palaeopathological analyses. Trabecular bone has been preserved (i.e., joint surfaces intact, and ribs, vertebrae and pelves are well represented).

Secondly, the surface preservation of the cortical bone was assessed following McKinley (2004, 16), who provides scores ranging between 0 (excellent) to 5+ (poor) to describe the postmortem modification of the outermost surface of cortical bone. Lastly, the degree of completeness of each individual was made based on estimations of the percentage of expected number of skeletal elements present for analysis, and allocated to the broad categories of <25%, 25%-50%, 50%-75% and 75%.

3.1.2 Biological sex and age-at-death

To maximise the accuracy of osteological assessments, it is necessary to analyse as many different skeletal regions as possible to understand trait variation both within and between individuals. The assessment of age-at-death in non-adults relies on the extent of skeletal maturation and dental development, and this was carried out according to Cunningham et al. (2016) and AlQahtani (2010), respectively. Each child was then assigned to one of seven broad age categories to permit comparison of individuals: perinate (i.e., died at or around the time of birth), 0-1 year, 1.1-2.5 years, 2.6-6.5 years, 6.6-10.5 years, 10.6-14.5 years, and 14.6-17.9 years. Prior to puberty, the macroscopic assessment of biological sex from the skeleton is challenging, and has not been explored during this analysis. Where possible, the stage of puberty for adolescents was also recorded, following Lewis et al. (2016) and Lewis and Falys (2020).

Once the skeleton and dentition are fully developed, standardized osteological methods for biological sex and adult age-at-death estimation rely on the morphology of the cranium, mandible and pelvis following Buikstra and Ubelaker (1994), and the distal humerus (Falys et al. 2005). In addition, metrical analysis of the maximum diameters of the humeral and femoral heads was undertaken following Stewart (1979), to permit comparison with the morphological expressions of biological sex. Individuals were categorised depending on the confidence of the biological sex assignment as: M (male), M? (probable male), I (indeterminate sex), F? (probable female), F (female).

An estimation of the age-at-death for adults was made based on dental wear (Brothwell, 1981), and degeneration of the auricular surface of the ilium (Lovejoy et al. 1985) and the pubic symphysis (Brooks and Suchey 1990) in the pelvis. Degeneration of the sternal end of the clavicle was also assessed for individuals aged 46+ years (Falys and Prangle 2015). Each individual was then assigned to one of four broad age categories that account for interpersonal variation in the ageing process: 18-25 years, 26-35 years, 36-45 years, 46+ years (Falys and Lewis 2011). Where no specific age category could be assigned, individuals were classified as 'non-adult' (<18 years) or 'adult' (18+ years).

3.1.3 Stature estimation

As 10% of attained adult stature is reliant on an adequate nutrition and freedom from infection during growth and development, the standing height of an individual can provide information on the environmental circumstances in which they grew up. These data can then be compared to means for males and females from other sites. Stature was estimated using the maximum length (cm) of intact long bones (preferably the femur) using regression equations provided by Trotter (1970).

3.1.4 Non-metric traits

Non-metric or epigenetic traits are variants in the morphology of the dentition and skeleton as the result of genetic or adaptational factors (Tyrell, 2000). They are recognised as additional creases or cusps in the teeth, extra projections of bone, foramina, sutures, facets or canals. These were classified according to Berry and Berry (1967) and Finnegan (1978), and illustrated by Brothwell (1981). Information on non-metric traits are detailed in the Skeleton Appendix only (Appendix 3). Further information is available on request.

4. Results

4.1 Surface preservation and completeness

Nearly half of the individuals in these phases of excavation were well preserved, with more than 75% of the skeleton available for analysis (n=19, 47.5%). Nine individuals (22.5%) were estimated to be between 50-75% complete, which was commonly due to the poor preservation of trabecular bone (i.e., vertebral bodies) and absence of small bones of the hands and feet. Nine individuals (22.5%) were between 25-50% complete, and three (7.5%, SK 2203, SK2204, and SK2509) were less than 25% complete, possibly the result of younger age in shallow burials (i.e. SK2203 and SK2204), or significant truncation (SK2509).

A total of 16 individuals (40.0%) had excellent (Grade 1) surface preservation, while 12 (32.5%) displayed patches of more severe surface erosion (Grade 2). Seven (17.5%) displayed more extensive surface erosion (Grade 3), and one (SK2536) had severe erosion (Grade 4). Three individuals displayed variable surface preservation (7.5%). SK2526 and SK2529 had Grades 2-3, and SK2520 was less well preserved, displaying Grades 3-4 (see Table 1).

4.2 Biological sex and age-at-death

The results of this stage of analysis are presented in Table 1 and Figure 4. The analysed individuals comprised 10 males (25.0%), 14 females (35.0%). In addition, three adult individuals (7.5%) were present for whom biological sex could not be confidently identified due to the skeletons displayed both male and female morphological characteristics (11.5%, SK2197, SK2199, and SK2502). The sample also included 13 children (32.5%) for whom a biological sex was not determined.

The non-adults were found to span much of childhood, with the exception that there were no non-adults aged 1.1-2.5 years or 14.6-17.9 years. The youngest individual (SK2531) from the 2024-5 excavations was aged 0-1 years (7.7% of all children). Most of the children were aged 2.6-6.5 years (n=5, 38.4%), four were 6.6-10.5 years (30.8%) and three were 10.6-14.5 years. It was possible to assess the stage of puberty for two of these individuals, SK2523 and SK2524, both of whom were aged 10.6-14.5 years and were in the acceleration phase of the adolescent growth spurt, meaning their bodies were gearing up for puberty by increasing bone and body mass, although they would still have appeared child-like.

The majority of the individuals (n=18, 66.7%) died in later life at over 46 years, with nearly double the number of females than males reaching advanced age (females, n=11, 61.1% of individuals aged over 46 years; males, n=6, 33.3%; indeterminate, n=1, 5.6%).

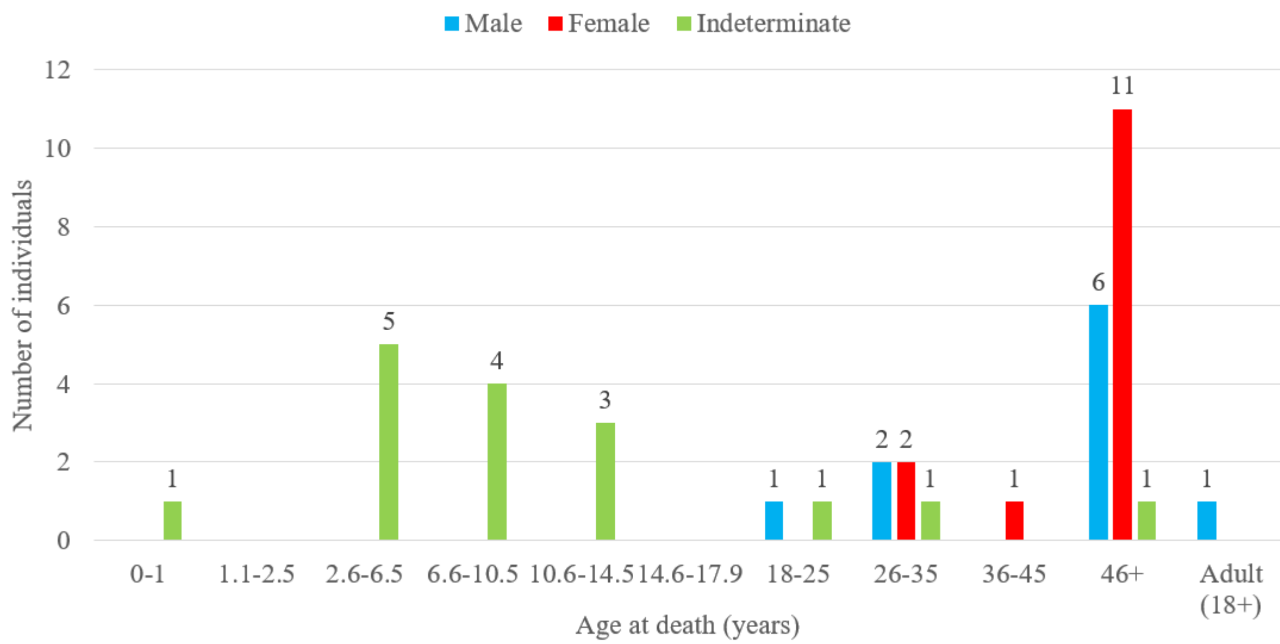

Figure 4. Distribution of biological sex and age-at-death of the 2024-5 individuals.

4.3 Stature

Stature was calculated for 11 of the 14 females who ranged in height between 151.7cm (SK2512) and 172.4cm (SK2515) (or 4'11½" to 5'7¾"), with an average of 161.7cm or 5'3¾" (Figure 5). Data was available for eight of the ten males with a range of 168.3cm (SK2500) to 175.9cm (SK2520) (or 5'6¼" to 5'9¼") and an average of 172.7cm (5'8"). Roberts and Cox (2003, 195) found a nearly equivalent average stature for both females and males in the early medieval period, with a female average of 161cm or 5'3" (152cm-170cm) and males measuring 172cm (5'7", with a range of 170cm-182cm). Data for the three adult individuals of indeterminate sex were not included in these analyses (i.e., SK2197, SK2199, and SK2502), but their estimated statures (if male or female) are provided in Table 1.

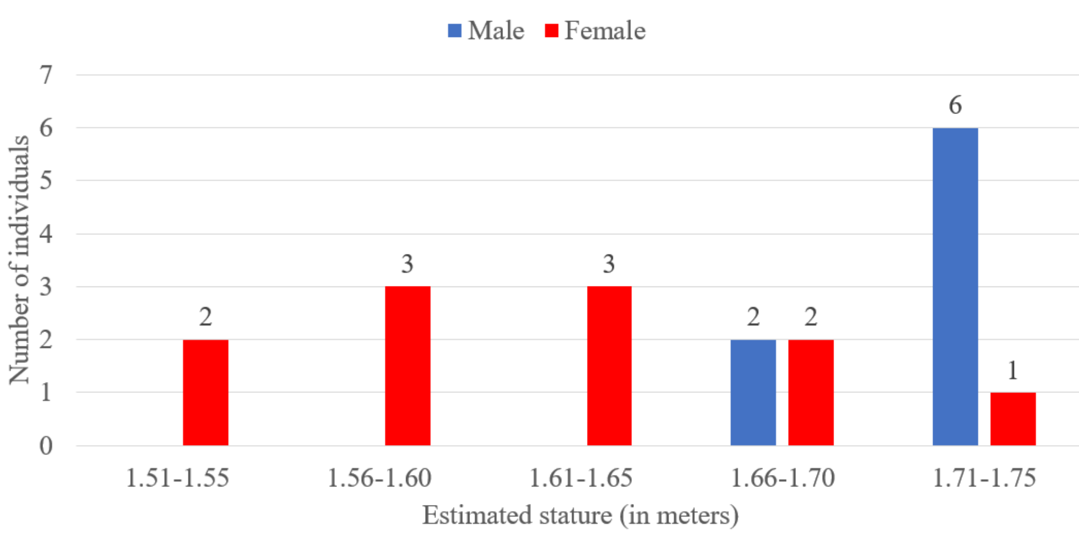

Figure 5. Estimated stature (in meters) for males and females excavated during 2024-5.

Table 1. Summary of the 2024 and 2025 burials from Trench 2 (n=40)

Skeleton	% Complete (surface)	Biological sex	Age (years)	Stature	
				cm	Ft in
2024					
2197	75+ (1)	Indeterminate	46+	If male: 169.5cm ± 3.27cm (right femur) If female: 166.2cm ± 3.72cm (right femur)	5'6½" 5'5½"
2199	25-50 (1)	Indeterminate	17-25	If male: 175.2cm ± 3.27cm (right femur) If female: 172.2cm ± 3.72cm (right femur)	5'9" 5'7½"
2202	50-75 (2)	Male	46+	170.4cm ± 3.27cm (right femur)	5'7½"
2203	<25 (2)	n/a	2.6-6.5	N/A	N/A
2204	<25 (2)	n/a	2.6-6.5	N/A	N/A
2217	75+ (1)	Female	46+	167.5cm ± 3.72cm (right femur)	5'6"
2218	75+ (2)	Female	26-35	159.1cm ± 3.72cm (right femur)	5'2¾"
2500	75+ (2)	Male	46+	168.3cm ± 3.27cm (right femur)	5'6¼"
2501	75+ (3)	Female	36-45	163.3cm ± 3.72cm (left femur)	5'4"
2502	75+ (1)	Indeterminate	26-35	If male: 164.2cm ± 3.27cm (right femur) If female: 160.8cm ± 3.72cm (right femur)	5'4½" 5'3¼"
2503	75+ (1)	Female	26-35	163.3cm ± 3.72cm (left femur)	5'4"
2504	25-50 (2)	Female?	46+	154.4cm ± 3.72cm (right femur)	5'½"
2505	50-75 (1)	Female	46+	167.7cm ± 3.72cm (right femur)	5'6"
2506	75+ (2)	Female	46+	156.4cm ± 3.72cm (right femur)	5'¾"
2507	50-75 (2)	Female	46+	Not possible to estimate	N/A
2508	75+ (1)	n/a	10.6-14.5	N/A	N/A
2509	<25 (2)	Female	46+	162.4cm ± 4.30cm (left ulna)	5'4"
2510	25-50 (3)	Male??	46+	Not possible to estimate	N/A
2511	75+ (1)	Male	26-35	171.4cm ± 3.27cm (right femur)	5'7½"
2512	25-50 (2)	Female??	46+	Approx 151.7cm ± 4.30cm (left ulna)	N/A
2513	50-75 (3)	N/A	6.6-10.5	N/A	N/A
2514	75+ (2)	Male	26-35	174.2cm ± 3.27cm (left femur)	5'8½"
2515	75+ (3)	Female	46+	172.4cm ± 3.72cm (right femur)	5'7¾"
2516	25-50 (1)	Female	46+	Not possible to estimate	N/A
2517	25-50 (3)	Male	46+	Approx. 174.7cm ± 3.27cm (left femur)	5'8½"
2519	50-75 (2)	N/A	2.6-6.5	N/A	N/A
2025					
2520	25-50 (3-4)	Male	18+	175.9cm ± 3.27cm (right femur)	5'9½"
2521	50-75 (3)	Male	46+	173.5cm ± 3.27cm (right femur)	5'8¼"
2522	25-50 (3)	N/A	6.6-10.5	N/A	N/A
2523	75+ (1)	N/A	10.6-14.5	N/A	N/A
2524	75+ (1)	N/A	10.6-14.5	N/A	N/A
2525	50-75 (1)	N/A	2.6-6.5	N/A	N/A
2526	25-50 (3)	N/A	2.6-6.5	N/A	N/A
2527	75+ (1)	N/A	6.6-10.5	N/A	N/A
2529	50-75 (2-3)	Male	18-25	Not possible to estimate	N/A
2530	75+ (1)	Female	46+	Not possible to estimate	N/A
2531	50-75 (1)	N/A	0-1	N/A	N/A
2534	75+ (1)	Female?	46+	160.8cm ± 3.72cm (right/left femur)	5'3¼"
2536	25-50 (4)	N/A	6.6-10.5	N/A	N/A
2537	75+ (1)	Male	46+	173.3cm ± 3.27cm (right femur)	5'8¼"

5. Health Status

Skeletal pathology can provide information on living conditions, diet, occupation, access to medical care, as well as numerous other aspects of everyday life of past populations (Roberts 2009). Pathological changes observed for the 2024-5 burials were classified into broad categories of pathology: dental disease (e.g., caries, calculus, periapical lesions, periodontal disease, antemortem tooth loss, linear enamel hypoplasia, and other dental anomalies), antemortem trauma (i.e., healed or healing injuries), congenital and developmental anomalies (e.g., supernumerary vertebrae, spina bifida occulta, lumbarisation, spondylosis, abnormal vertebral development), degenerative joint disease (including osteoarthritis and Schmorl's nodes). The less frequently occurring pathologies were infectious disease (i.e., specific and non-specific infection), circulatory disruptions (e.g., osteochondritis dissecans), possible evidence of perimortem trauma (i.e., trauma occurring at or around the time of death), and suspected neoplastic diseases (e.g., cancers). Skeletal and dental pathology was assessed following criteria set out in Buikstra (2019). A summary of the pathological conditions of each individual is provided in Appendix 1, as well as additional photographs in Appendix 3 (Skeleton Catalogue).

5.1 Dental health

Teeth can provide information on more than just oral hygiene. Dental disease reflects the quality of the diet and the enamel on tooth crowns can record periods of illness or malnutrition during childhood (Roberts et al. 2026). Dentition was available for 36 of the 40 individuals, the exceptions were SK2504, SK2509, SK2513 and SK2520 who have yet to be completely excavated. A total of 518 adult (permanent) teeth were present (217 maxillary, 301 mandibular), and 119 deciduous teeth (55 maxillary and 64 mandibular). A total of 740 tooth sockets were preserved, although much fragmentation of the alveolar bone was noted, ultimately resulting in the postmortem loss of 143 teeth. Overall, the dentition was well preserved, which permitted investigations of the prevalence of antemortem tooth loss, caries (cavities), calculus (plaque deposits), periapical lesions (e.g., abscesses), alveolar resorption (gingivitis), and enamel hypoplasia. Crude (CPR) and true prevalence rates (TPR) of dental disease are provided where possible, and a summary of dental disease for the 2022-3 and 2024-5 seasons is provided in Appendix 2.

5.1.1 Antemortem tooth loss (AMTL)

The loss of teeth before death can result from many reasons, including severe dental attrition, caries, periodontal disease, abscesses, advancing age, and are characterized by healing of the tooth socket (Roberts et al. 2026, 72). In total, 16 of 24 adult individuals (CPR= 66.7%) lost at least one tooth prior to death. Of the 740 adult tooth sockets present for analysis, 79 displayed antemortem tooth loss (TPR=10.7%). Perhaps as to be expected, all individuals were aged 46+ years, with the exception of SK2501 (female, 36-45 years) and SK2514 (male, 26-35 years). Between 1 and 14 teeth were lost. Roberts and Cox (2003, 191-193) found a crude prevalence rate of 3.1% and a true prevalence rate of 8.0% for antemortem tooth loss in early medieval Britain.

5.1.2 Dental caries

Caries are progressive diseases during which bacteria contribute to the erosion and destruction of tooth crowns and/or roots, commonly associated by acids that develop from the bacterial fermentation of food sugars (e.g., sucrose). A total of eight individuals (CPR = 8/36; 22.2%) displayed between one and four (SK2203 and SK2514) carious lesions (n=17/563 teeth, TPR = 3.0%). Roberts and Cox (2003, 190-191) found a CPR of 5.2% and TPR of 4.2% for the whole of the early medieval period.

5.1.3 Calculus

Calculus is the mineralization of dental plaque that collects on the surfaces of the tooth crowns. Daily brushing of teeth removes plaque before it can calcify, so the presence of calculus indicates that dental hygiene was not a daily priority. Archaeologically, calculus deposits are most commonly identified on the buccal (cheek) and lingual (tongue) surfaces of the dentition. Occasionally calculus deposits can be present on the occlusal surfaces of teeth (i.e., the biting surfaces), either unilaterally (one sided), or bilaterally, which would indicate the individuals was not actively chewing food (or other materials) on the affected side(s) of the mouth (Roberts et al. 2026).

Deposits of dental calculus were observed on the dentition of 17 individuals (n=17/36, CPR=47.2%). The severity of calculus deposits was scored following Brothwell (1981) as slight, medium or considerable. One individual, a 46+ year-old female (SK2516) displayed considerable calculus on the buccal surfaces of the maxillary molars. The CPR rate of 47.2% is slightly high compared to that provided by Roberts and Cox (2003, 190-194) for early medieval England, at 39.2%. Of the 17 individuals with calculus, five also displayed thin layers of calculus within the wear facets on the occlusal surfaces of the dentition (most commonly the molars), indicating food was not being actively chewed on one or more sides of the mouth for a period of time (n=5/36, CPR=13.9%). This could be the result of either pain due to an existing abscess or temporo-mandibular joints diseases, or as the result of paralysis, perhaps from a stroke. No clear reasons for the occlusal calculus were evident in these individuals.

5.1.4 Periapical lesions

Periapical lesions (abscesses, granulomas, cysts) result from bacteria entering the roots or pulp cavities of teeth. Caries, trauma, and severe wear all provide the openings in dental enamel that give rise to these lesions. Pain and characteristic holes in the surrounding jaw are formed, and for abscesses involves pus that can exude through the bone (Dias and Tayles, 1997). Two mature individuals had well-defined holes observed in their jaws, associated with the first molars, likely the result of severe wear to the crowns (n=2/36, CPR=5.6%). Roberts and Cox (2003, 191-192) found the TPR of periapical abscesses in early medieval England to be 2.8% (CPR=3.9%).

5.1.5 Periodontal disease

Commonly known as gingivitis or gum disease, periodontal disease is the chronic inflammation of the soft tissue of the gums. Ultimately, the chronic inflammation gradually resorptions the alveolar bone of the maxilla and/or mandible. As the alveolar bone recedes, antemortem tooth loss can result, as the roots of the dentition become less and less anchored in the bone (Roberts et al. 2026, 71). The degree of resorption of the alveolar bone was graded following Brothwell (1981) as slight, medium and considerable. Twenty-three adults had jaws preserved well enough for observation and 20 (CPR=87.0%) displayed some degree of alveolar resorption. Of these, 10 individuals displayed "slight" resorption, six displayed "medium" and four displayed "considerable" periodontal disease.

5.1.6 Enamel hypoplasia

Enamel hypoplasia are linear defects of the enamel that are formed in response to nutritional deficiency or pathological events (e.g., acute illness, high fever) during childhood. While the crowns are developing within the jaws (commonly under the age of 7 years), these episodes of disease or malnutrition cause a cessation of growth in order to re-direct the body's energy into healing the physiological stress, resulting in deficiencies of the enamel (Roberts et al. 2026, 73). The presence of enamel defects (clear horizontal linear defects) was recorded on the anterior dentition of 34 individuals, and 20 (CPR=58.8%) were affected, signifying that they survived period(s) of illness/systemic childhood stress.

5.1.7 Other dental observations

In addition to the common dental diseases, discussed above, other dental observations were recorded included unusual patterns of dental wear and tooth positions. For example, the mandibular canines of SK2521 (M, 46+ years) were rotated, and the right mandibular incisors of SK2529 (M, 17/25 years) were overcrowded, so the right lateral incisor was pushed to a position behind the central incisor and canine.

Unexpected patterns of wear were noted in six individuals, including considerable wear of the anterior teeth (maxillary and mandibular) and right mandibular molars in SK2521 (M, 46+ years), wear facets on anterior mandibular canine crowns in SK2527 (6.6-10.5 years), considerable horizontal wear to the mandibular anterior dentition of SK2530 (F, 46+ years) and SK2534 (F, 46+ years), wear to deciduous canines of SK2536 (6.6-10.5 years), and cupped wear on canines and premolars, slanted wear (lingual surfaces) on third molars in SK2537 (M, 46+ years).

5.2 Congenital and developmental anomalies

Such conditions can occur anywhere in the skeleton, and result from genetic factors, such as poor maternal health (e.g., virus infection, poor diet), environmental pollution or trauma in the womb. Congenital conditions that severely affect the growth and/or development of the baby would have resulted in the death of the individual before or at birth, making them invisible in the archaeological record (Roberts et al. 2026, 37). Of the 30 individuals aged over 10.6 years (where these changes are more readily observed), six (CPR=20.0%) displayed developmental anomalies (Table 2). SK2503 (F, 26-35 years, Figure 6) had four different skeletal changes. Two individuals had a lumbarised 12th thoracic vertebra (this common vertebral border shift would have been asymptomatic) and two had spondylolysis (both CPR=6.7%). Spondylolysis describes the non-union of the arch to the vertebral body, or its later detachment, possibly the result of a repetitive stress (e.g., bending and lifting) applied to a hereditary weakness rather than an acute traumatic event (Buikstra 2019). Spondylolysis most commonly affects the fourth and fifth lumbar vertebrae and a symptom of this condition is lower back pain.

Table 2. Individuals with congenital or developmental anomalies.

Anomaly	Skeleton	Biological sex	Age (years)	Notes
Lumbarisation of T12	2515	Female	46+	
Lumbarisation of T12	2523	Non-adult	10.6-14.5	
6th lumbar vertebra	2503	Female	26-35	
Spina bifida occulta	2523	Non-adult	10.6-14.5	
Spondylolysis	2500	Male	46+	L5
Spondylolysis	2503	Female	26-35	L6
Unfused transverse process	2218	Female	26-35	
Cleft vertebral body	2503	Female	26-35	L3 and L5
Cleft neural arch	2523	Non-adult	10.6-14.5	S2 and S3
Perthes disease?	2503	Female	26-35	
Bipartite medial cuneiforms	2511	Male	26-35	

Figure 6. Possible development defects of SK2503. Midline cleft defects of anterior body of L3 and L5 (arrowed) (left), and flattened femoral heads (posterior view), right.

Further analysis is needed for two individuals for possible congenital/developmental conditions. These individuals were buried immediately adjacent to one another. SK2502 (I, 26-35 years), had a mixture of cranial and postcranial sexually dimorphic traits, and notable short and stocky morphology of the limb bones. SK2511 (M, 26-35 years) in addition to bipartite medial cuneiforms, the humeri were straight and asymmetrical, suggesting paralysis of the left arm, with deep intertubercular grooves (Figure 7), strong scapular muscle attachments, abnormal raised ridges on distal/anterior/lateral femora (proximal femora are broad and flat), pronounced ridges along proximal/posterior tibiae (joining to spiral line), and the fibulae are of different curvatures. While these observations may be of normal skeletal variation, it may also be possible they are the result of a congenital/developmental condition.

Figure 7. SK2511: straight humeri, with deep intertubercular grooves on the proximal ends (left), and abnormal fusion of the medial cuneiforms (right).

5.3 Trauma

Skeletal trauma can occur accidentally or intentionally, as the result from cultural practices or therapeutic/surgical intervention (Cuhna and Pinheiro 2009). Traumatic wounds (e.g., fractures, trepanations, weapon trauma, dislocations, haematomas) may result in the damage of soft tissue and bone. Trauma is categorised as either antemortem and perimortem, the differentiation between the two depending on the timing of the injury. Antemortem wounds are inflicted some time before death allowing for healing to commence (i.e., callus formation, rounded lesion margins). Perimortem trauma is inflicted at or very close to the time of death. These injuries are characterized by sharp and irregular margins, completely devoid of healing. Further investigations (e.g., radiographs) are required to confirm the nature of the trauma described below.

5.3.1 Antemortem trauma

In total, 19 individuals (CPR=47.5% of all burials or 70.4% of adult individuals) had evidence of antemortem skeletal trauma (Table 3). Figure 8 presents the distribution of antemortem trauma by region. The spine was most commonly affected (n=8/23, CPR=34.8%), followed by the forearms/wrists (n=6/24, CPR=24.0%), and legs (n=6/25, CPR=24.0%). Macroscopic examination indicates significant remodelling, however, radiographs are required to record the exact extent of the healing.

In modern medicine, fractures may be "reduced" (either pulled back into alignment or surgically fixed with plates and screws) to ensure minimal physical complications or deformity throughout the healing process. Three injuries at Cookham highlight the importance of reducing fractures, and what can happen if it is not undertaken. Bilateral fractures of the forearms were observed for a 46+ years male (SK2202), however, the left side displayed the most significant fractures. Perhaps as the result of a fall from height, the lack of reducing or splinting the forearm resulted in the non-union of the distal third of the ulnar shaft, and the distal radius was displaced and fused at nearly a 90° angle (Figure 9a). The left forearm would have shown a considerable deformity, and it is likely use of the left hand would have been severely limited. A mature probable female (SK2504) sustained an oblique fracture of the right distal tibia and fibula (just above the ankle). The fracture fragments were forced upwards and healed in that position, ultimately shortening the right lower leg by over 3cm (right=31.3cm, left=34.4cm) (Figure 9b). This woman would likely have walked with a pronounced limp. Finally, another mature female (SK2530) had multiple antemortem injuries. These affected the left shoulder blade, the right side of the first and second cervical vertebrae, fusion (ankylosis) of the sixth and seventh thoracic vertebral bodies, spondylolysis of the fifth lumbar vertebra, a fracture of the right femoral neck (Figure 9c), and probable traumatic ankylosis of the second and third metatarsals to the proximal phalanges in the left foot, which fixed the second and third toes in a permanent dorsiflexed position. Following the fracture of the right femoral neck, the femoral head/neck healed in an inferior angle to the normal element. This would have severely affected the mobility of the right hip joint, and it is possible that this female had limited weight bearing on her right leg. A conclusion supported by the slight atrophy of the right femur compared to the left. It is also possible that her shoulders had subluxated posteriorly resulting in osteoarthritis of the ventral surfaces of the acromia of the scapulae.

Not visible as broken bones, the legs of child SK2513 had premature fusion of the distal femoral epiphysis of the right leg, and the proximal epiphysis of the left tibia. Both occurrences would have inhibited the right femur and left tibia from reaching their maximum growth potential, leading to stunted growth of those elements. The skull and upper chest of SK2513 were not excavated as they were situated beneath the western baulk of Trench 2. The bilateral pattern of the fusion is unusual but may have occurred due to a fall from a height onto the legs.

Table 3. Antemortem trauma in the 2024-5 burials.

Skeleton	Biological sex	Age (years)	Bone(s) affected		Status of healing
			Side	Location	
2218	Female	26-35	Left	Radius, distal end (Colles')	Healed
			Right	Radius, distal end (Colles')	Healed
2202	Male	46+	Left	Radius, midshaft	Healed, mal-aligned (90°)
			Left	Ulna, midshaft	Healed, non-union
			Right	Radius, distal	*
			Right	Ulna, distal	*
2500	Male	46+	Left	Clavicle, midshaft	Healed, mal-aligned
2501	Female	36-45	Left	Parietal, posterior to temporal line	Healed
			Right	Radius, distal end (Colles')	Healed*
2504	Female?	46+	Right	Tibia, distal third of shaft	Healed, with ankylosis to fibula
			Right	Fibula, distal third of shaft	Healed, with ankylosis to tibia
			Bilateral	Lumbar vertebrae neural arches	**
2506	Female	46+	Midline	L2 (inferior) and L3 (superior)	**
			Midline	Sacrum	Healed
2507	Female	46+	Right	L3 (inferior) and L4 (superior) body surfaces	Erosive lesions (inflammation)
2511	Male	26-35	Midline	T7-T9 bodies	Anterior wedging of T7-T9 bodies**
			Midline	L3-L5 bodies	Intervertebral osteochondrosis**
2512	Female?	46+	Left	Ulna, distal end	Possible, healed*
			Left	Tibia, midshaft	Possible, healed*
			Left	Fibula, midshaft	Possible, healed*
2513	Non-adult	6.6-10.5	Right	Femur, distal (premature epiphyseal fusion	
			Left	Tibia, proximal (premature epiphyseal fusion)	
2514	Male	26-35	Right	Proximal manual phalanx, distal end	Trauma or arthropathy**
			Right	5th metatarsal, head Proximal pedal phalanx, proximal end	Trauma or arthropathy**
			Midline	Throughout spine	
			Midline	Lumbar vertebral bodies	**
2515	Female	46+	Left	Clavicle, lateral midshaft	Healed
2516	Female	46+	Left	Scapula, blade	Possible, healed*
2517	Male	46+	Left	Femur, neck	Healed
2521	Male	46+	Right	Femur, neck	Healed
2523	Non-adult	10.6-14.5	Right	Clavicle, lateral/superior	Fracture or non-metric trait**
2530	Female	46+	Left	Scapula, spine	
			Bilateral	Scapulae (subluxed shoulders)	
			Right	Vertebrae, C1/C2 facets	
			Bilateral	Vertebrae, T6-7? bodies	Ankylosis
			Right	Femur, neck	
			Left	Foot: MT2 and MT3	Ankylosis with proximal phalanges

Table 3 (continued). Antemortem trauma in the 2024-5 burials.

Skeleton	Biological sex	Age (years)	Bone(s) affected		Status of healing
			Side	Location	
2534	Female	46+	Right	Mandible (anterior dislocation)	
			Right	Ischium	Non-fusion of upper ischial tuberosity
			Bilateral	Radii	*
			Right	Tibia and fibula, distal	
			-	T11/T12 bodies (depressions)	
2537	Male	46+	Left	Mandible (projection)	
			Bilateral	Radii, distal	*
				Vertebrae, C2/C3	Ankylosis

*radiograph required; **to be confirmed

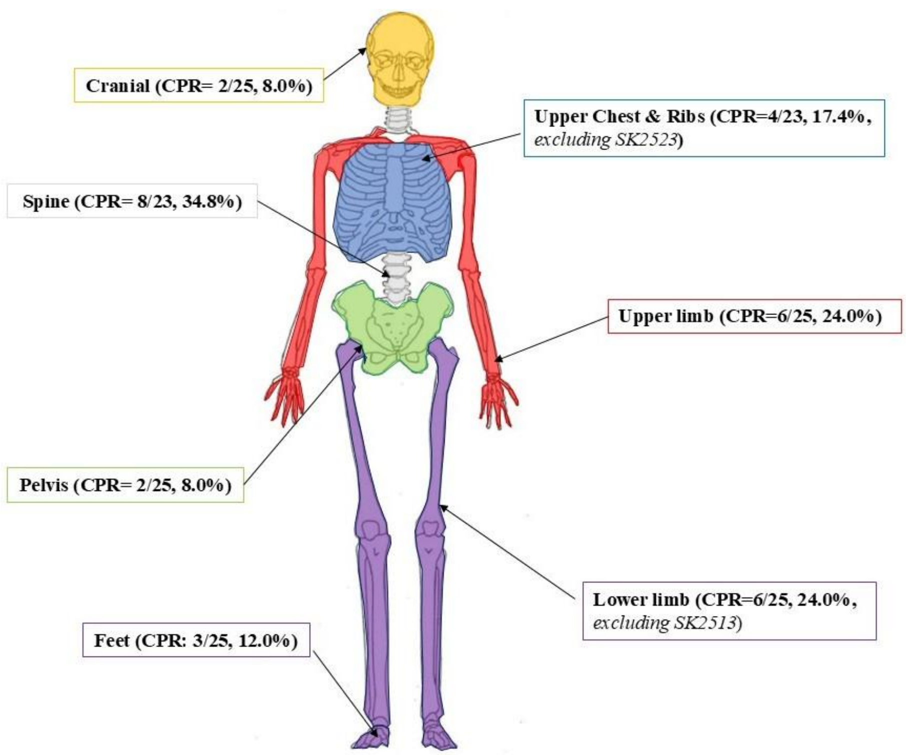

Figure 8. Distribution of antemortem fractures of the 2024-5 individuals.

Figure 9. Examples of healed antemortem trauma: left forearm of SK2202 with non-union of ulna and malalignment of the radius (a), the tibiae and fibulae of SK2504 with subsequent ankylosis (b), and the right proximal femur of SK2530 (c)

5.3.2. Perimortem trauma

Possible perimortem injuries were observed in two individuals (CPR=5.0%), but more analysis is needed to confirm their diagnosis. They are highlighted here to aid further investigations. These include a 2.6-6.5 year old (SK2526) has a possible linear sharp-force injury on the left side of their forehead, and SK2537 (M, 46+ years), who has a possible sharp-force injury to the superior aspect of the patellar surface of the right distal femur (patellar surface).

5.4 Degenerative joint disease

Degenerative joint disease is the gradual deterioration of the joints of the body, characterised by features such as the development of marginal osteophytes, porosity, and ultimately, joint surface contour change. Its presence signifies that biomechanical wear and tear have been placed on the joints of the skeleton, which commonly accumulate over a life time (i.e., linked to advancing age), although can also form in response to trauma. Symptoms, depending on degree of arthritis, can be impairment of movement and/or pain. Osteoarthritis is a form of degenerative joint disease that only affects the synovial joints (Roberts et al. 2026, 153). It most commonly affects the weight-bearing joints of the body, although any synovial joint can be affected. Osteoarthritis manifests itself in three ways: osteophytes, surface contour change, porosity, and/or eburnation (polishing of the bone from bone-on-bone contact). Waldron and Rogers (1991) suggest that eburnation is the most diagnostic feature of osteoarthritis, and if this is not present, the other three criteria must be evident for a diagnosis of osteoarthritis.

As expected due to the high frequency of older individuals at the site, 22 of the 27 adults suffered from degenerative joint disease (CPR=81.5%, Table 4). Nine individuals had Schmorl's nodes (n=9/24, CPR=37.5%) with nearly equivalent numbers of males (n=3) and females (n=4) affected. Schmorl's nodes result from physical pressure on the developing spine, normally during adolescence (Kyere et al. 2012; Roberts et al. 2026, 157). They are generally asymptomatic, but if centrally located, can result in back pain. Roberts and Cox (2003, 198) reported a CPR of 24.7% for Schmorl's nodes in the early medieval period.

Table 4. Crude prevalence rate of degenerative joint disease

Joint affected	Males (n=10)			Females (n=14)			Indeterminate (n=3)		
	n	Affected	CPR (%)	n	Affected	CPR (%)	n	Affected	CPR (%)
TMJ	9	0	0	13	1	7.7	3	0	0
Spine	7	5	71.4	14	9	64.3	3	2	66.7
Schmorl's nodes	7	3	42.9	14	4	28.6	3	2	66.7
Right shoulder	9	2	22.2	14	3	21.4	3	0	0
Left shoulder	9	3	33.3	13	2	15.4	2	0	0
Right elbow	9	2	22.2	13	4	30.8	3	0	0
Left elbow	9	2	22.2	13	2	15.4	2	0	0
Right wrist/hand	9	2	22.2	13	1	7.7	3	0	0
Left wrist/hand	9	1	11.1	13	3	23.1	2	0	0
Right hip	8	4	50.0	13	8	61.5	3	0	0
Left hip	9	3	33.3	13	8	61.5	2	0	0
Right knee	10	1	10.0	13	2	15.4	3	0	0
Left knee	10	2	22.2	13	1	7.7	2	0	0
Right ankle/foot	10	1	10.0	13	1	7.7	3	0	0
Left ankle/foot	10	1	10.0	13	2	15.4	3	0	0

5.4.1 Osteoarthritis

Six older (46+ years) individuals (CPR=22.2%) had eburnation of their joints (Table 5): on the left articular facets of C6/C7 (neck vertebrae), the right distal radius and ulna, and right knee of SK2202, the left hips of three males (SK2517, SK2521, and SK2537), the left articular facet of the axis (C2) in SK2505, the right articular facets in T3/T4 of SK2521, and the anterior surfaces of the acromia and the spine in SK2530.

Table 5. Crude prevalence rate of osteoarthritis in the adult 2024-5 burials (n=27)

Joint affected	Males (n=10)			Females (n=14)			Indeterminate (n=3)		
	n	Affected	CPR (%)	n	Affected	CPR (%)	n	Affected	CPR (%)
TMJ	9	0	0	13	0	0	3	0	0
Spine	7	2	28.6	14	2	14.3	3	0	0
Right shoulder	7	0	0	13	1	7.7	3	0	0
Left shoulder	9	0	0	13	1	7.7	3	0	0
Right elbow	9	0	0	13	0	0	2	0	0
Left elbow	9	0	0	13	0	0	3	0	0
Right wrist/hand	9	1	11.1	13	0	0	2	0	0
Left wrist/hand	9	0	0	13	0	0	3	0	0
Right hip	8	1	12.5	13	0	0	2	0	0
Left hip	9	3	33.3	13	0	0	3	0	0
Right knee	9	1	11.1	13	0	0	2	0	0
Left knee	10	1	10.0	13	0	0	3	0	0
Right ankle/foot	10	0	0	13	0	0	2	0	0
Left ankle/foot	10	0	0	13	0	0	3	0	0

5.5 Infections

In palaeopathology, infectious diseases fall into two categories, non-specific infections, where the pathogen is unknown, and those with a specific cause (e.g., leprosy, treponemal disease, tuberculosis). Non-specific infections result from unknown pathogens, and can manifest in the inflammation of three different aspects of a bone: sub-periosteal new bone formation affects the fibrous sheath (periosteum) that covers the outermost layer of a skeletal element, osteitis is the inflammation of the cortical bone (the thick, dense external layer of bone), and osteomyelitis, which results from infection deep within the medullary cavity (Roberts et al. 2026).

5.5.1 Sub-periosteal new bone formation (SPNB)

Identified as plaques of porous, grey or light brown woven (or fibre) bone on the surface of the cortical bone, sub-periosteal new bone indicates the bone was actively remodelling at the time the individual died. As the remodelling process progresses, the woven appearance of the initial fibre bone takes on a smoother, denser textured bone (lamellar), which indicates the condition was present for some time prior to death, and the body had time to start the healing process. In total, 24 individuals (n = 24/40, CPR=60.0%) displayed periosteal reaction (Table 6). Four specific patterns of non-specific infection were noted, affecting the cranium (endocranial lesions), the chest, and the lower legs. Endocranial lesions were noted in 5 individuals of varying ages (n=5/34, CPR=14.7%). Seven individuals had new bone in the maxillary or frontal sinuses, indicative of sinusitis (n=7/38, CPR=18.4%). Three individuals had visceral rib lesions indicative of an active chest infection (n=3/39, CPR=7.7%). In SK2527, a 6.6-10.5 year-old, the lesions may be related to tuberculosis (see below). Finally, the lower limbs (primarily the tibial shafts) of seven individuals displayed SPBN that had progressed well into the healing process, displaying porous and striated lamellar bone (n=7/40, CPR=17.5%). The shins are a common place for SPNB, due to the lack of thick muscle along the anterior surface of the tibia, and as a result, bumps and knocks to the shins can result in SPNB, although a preponderance of new bone on the distal aspect of the tibia is less common.

One child (SK2204, 2.6-6.5 years) had a lytic lesion (cloaca) on the right external auditory meatus, possibly the result of drainage from an inner ear infection (Figure 10).

Figure 10. Lytic lesion to inferior external auditory meatus of the right temporal bone (ear) of SK2204.

Table 6. Distribution of active new bone formation in the 2024-5 burials.

Skeleton	Biological sex	Age-at-death (years)	Cranium	Chest	Spine	Pelvis	Upper limb		Lower limb	
							Humerus	Forearm/ hands	Femur	Lower leg/ feet
2199	Indeterminate	17-25	Yes							
2217	Female	46+		Yes						Yes
2500	Male	46+								Yes
2501	Female	36-45	Yes							
2503	Female	26-35							Yes	Yes
2505	Female	46+	Yes							
2506	Female	46+								Yes
2510	Male?	46+	Yes							
2511	Male	26-35								Yes
2512	Female?	46+								Yes
2513	Non-adult	6.6-10.5							Yes	Yes
2514	Male	26-35	Yes	Yes						
2515	Female	46+	Yes							Yes
2516	Female	46+					Yes			
2520	Male	18+							Yes	Yes
2522	Non-adult	6.6-10.5	Yes							
2523	Non-adult	10.6-14.5								Yes

Skeleton	Biological sex	Age-at-death (years)	Cranium	Chest	Spine	Pelvis	Upper limb		Lower limb	
							Humerus	Forearm/ hands	Femur	Lower leg/ feet
2524	Non-adult	10.6-14.5	Yes							Yes
2526	Non-adult	2.6-6.5	Yes							
2527*	Non-adult	6.6-10.5	Yes	Yes		Yes			Yes	
2529	Male	17-25	Yes							
2530	Female	46+	Yes							
2531***	Non-adult	0-1	Yes							
2537	Male	46+								Yes

5.5.2 Specific infection

Of the 24 individuals displaying locations of sub-periosteal new bone formation, two children, each aged 6.6-10.5 years, had lesions that suggested they had suffered from a specific condition, possibly tuberculosis (2/40, 5.0%). SK2522 and SK2527 both had cranial lesions suggestive of TB, including granular lesions (SK2522), and increased vascular impressions, and endocranial lesions (SK2527). The postcranial skeleton of SK2527 also displayed diffuse sub-periosteal new bone formation on the visceral surfaces of the ribs, the ilia, and femora (Appendix 3).

5.6 Indicators of non-specific stress

Cribra orbitalia is a common palaeopathological condition that has been traditionally linked to iron-deficiency anaemia, either through malnutrition, parasitic infection, or excessive blood loss (Roberts et al. 2026). Walker et al. (2009) suggested that it may be the result of megaloblastic anaemia resulting from a deficiency of vitamins B12 and B9. These vitamins are found in animal products such as fish, leafy vegetables, cheese, eggs, and red meat. Nine out of 38 individuals with orbits (CPR=23.7%) had cribra orbitalia. Roberts and Cox (2003) reported a CPR of 7.6% for early medieval England. Two individuals, a 26-35 year-old female (SK2503) and a 6.6-10.5 year-old child (SK2513) had cribra femoralis (porous lesions on the proximal femur). A recent study suggests that rather than a pathological process, these lesions are linked to age-at-death, and formed during the normal growth process (Schatz, 2021).

5.6.1 Limb asymmetry

Another possible indication of systemic stress is the asymmetry of the long bones. Although limb-length is influenced by genetics, they can also be affected by environmental and biomechanical factors. For example, length and robusticity the humerus and clavicle may suggest, as the dominant arm would be more frequently used for tasks for the overall length and robusticity would be larger than the non-dominant arm (Zelazny et al. 2021). Environmental stresses, such as malnutrition, excessive noise, cold and heat can also enhance long bone asymmetry. Pathological conditions may be identified if side differences are pronounced. Table 7 summarises the maximum lengths of the humeri and femora (cm), where suitably preserved, as well as the calculated difference in length between the left and right sides (left (cm) – right (cm) = long bone length difference in cm). Resultant differences with negative results indicate the right side was longer than the left.

Asymmetry of the humerus or femur could be assessed for 12 individuals, with nine individuals having both elements preserved for comparison. The humerus displayed greater asymmetry than the femur. The most marked asymmetry was found in two mature females (SK2217 and SK2534) who had differences of 0.9cm and 1.0cm between the humeri, respectively. The largest difference between femora was found in a 26-35 year-old male (SK2514) whose right femur was 0.9cm longer than the left. Significant differences between the lengths of the leg bones may suggest the individual would have walked with a limp.

Table 7. Maximum length (cm) of the left and right humeri and femora

Skeleton	Biological Sex	Age (years)	Humerus			Femur			Stature
			Left	Right	Diff.	Left	Right	Diff.	
2217	Female	46+	31.7	32.6	-0.9	45.5	45.9	0.4	167.5cm ± 3.72cm
2218	Female	26-35	30.3	30.6	-0.3	42.5	42.5	0.0	159.1cm ± 3.72cm
2500	Male	46+	-	-	-	44.9	44.9	0.0	168.3cm ± 3.27cm
2501	Female	36-45	31.8	31.7	0.1	44.2	44.1	0.1	163.3cm ± 3.72cm
2502	Indeterminate	26-35	29.8	30.2	-0.4	43.0	43.2	-0.2	If male: 164.2cm ± 3.27cm If female: 160.8cm ± 3.72cm
2503	Female	26-35	31.4	31.9	-0.5	44.2	43.8	0.4	163.3cm ± 3.72cm
2504	Female?	46+	-	-	-	40.4	40.6	-0.2	154.4cm ± 3.72cm
2506	Female	46+	28.9	28.9	0.0	41.2	41.4	-0.2	156.4cm ± 3.72cm
2511	Male	26-35	34.4	35.0	-0.6	46.3	46.2	0.1	171.4cm ± 3.27cm
2514	Male	26-35	34.2	34.7	-0.5	47.4	46.5	0.9	174.2cm ± 3.27cm
2520	Male	18+	-	-	-	47.9	48.1	0.2	175.9cm ± 3.27cm
2534	Female	46+	31.0	32.0	-1.0	43.2	43.2	0.0	160.8cm ± 3.72cm

Asymmetries of other limb bones were also noted in five individuals, including two young adolescents aged 10.6-14.5 years-old. Each had notable differences in the robusticity of the left and right humerus. The reason for the asymmetry in SK2202 is the significant fracture of the left forearm, for whom the subsequent malalignment of the bones of the left radius would have inhibited use of the left arm, leading to atrophy of the left humerus. It was not possible to suggest the cause of the upper limb asymmetry of the other three individuals.

5.7 Neoplastic disease

Neoplastic diseases are characterized as new or abnormal growths caused by uncontrolled growth of tissue cells (Roberts et al. 2026), although are more commonly known as cancer. Two categories of neoplasm exist: benign and malignant. Benign neoplasms do not tend to spread from their point of origin, or threaten life. Clinically, they are largely asymptomatic, and do not produce pain. In contrast, malignant cancers are characterized by uncontrolled growth and/or spread throughout the body via the blood stream, lymphatic system, or direct implantation of cells in organ tissues (Roberts et al. 2026). Metastases (secondary deposits) manifest themselves in organs, disrupting and breaking down the normal function, and resulting in death. Clinically, malignant cancers produce symptoms including weight loss, anaemia, and pain.

Nine individuals displayed lytic and/or blastic lesions on their cranial and postcranial bones that may be of neoplastic origin (n=9/40, CPR=22.5%). These include five individuals with cranial lesions (12.5%). Examples include a single benign neoplasm (a button osteoma) on the ectocranial surface of the frontal bone of SK2197 (I, 46+ years), a rounded, space-occupying lesion with a raised biological edge to the left of the midline of the left frontal bone (ectocranial) of SK2529 (M, 17-25 years), with an adjacent remodelled area superior to the blastic lesion, and a spiculated nodule on the endocranial surface on the midline of the frontal bone of SK2516 (F, 46+ years) (Figure 11a-c). It is noted that much more research in the form of a radiographic survey is needed to fully investigate the prevalence of cancer at the site.

Table 8. Cases (and possible cases) of neoplastic disease in the 2024/25 burials

Skeleton	Biological Sex	Age (years)	Skeletal element	Side/ location	Location of lesion(s)/ appearance
2197	Indeterminate	46+	Cranium: frontal bone	Right	Button osteoma on ectocranial surface
2501	Female	36-45	Leg: femur	Right	Lytic (?) depressions to anterior/medial shaft of left distal femur*
2502	Indeterminate	26-35	Leg: tibia	Right	Pedunculated osteochondroma (benign)
2505	Female	46+	Cranium: right parietal and occipital bones	Right	Erosive lesions on ectocranial surfaces, and within diploë*
2515	Female	46+	Cranium: Parietals	Bilateral	Erosive lesions
			Vertebral bodies	Thoracic and lumbar	
			Leg: femur	Right (distal)	
2516	Female	46+	Cranium: frontal bone	Midline/ endocranium	Spiculated nodule (does not look like classic HFI)
2524	Nonadult	10.6-14.5	Cranium: margin of right orbit	Midline	Space-occupying lesion
2529	Male	17-25	Cranium: frontal bone	Left	Rounded, raised lesion on left frontal bone (ectocranial), irregular flattened/smooth area superior to rounded lesion demarcated by ridges, porous lesion on left parietal bone with associated groove, possible space-occupying lesion on left posterior humerus shaft (distal third)
2530	Female	46+	Humerus	Right	erosive lesions on head of right humerus

*requires a radiograph to confirm diagnosis.

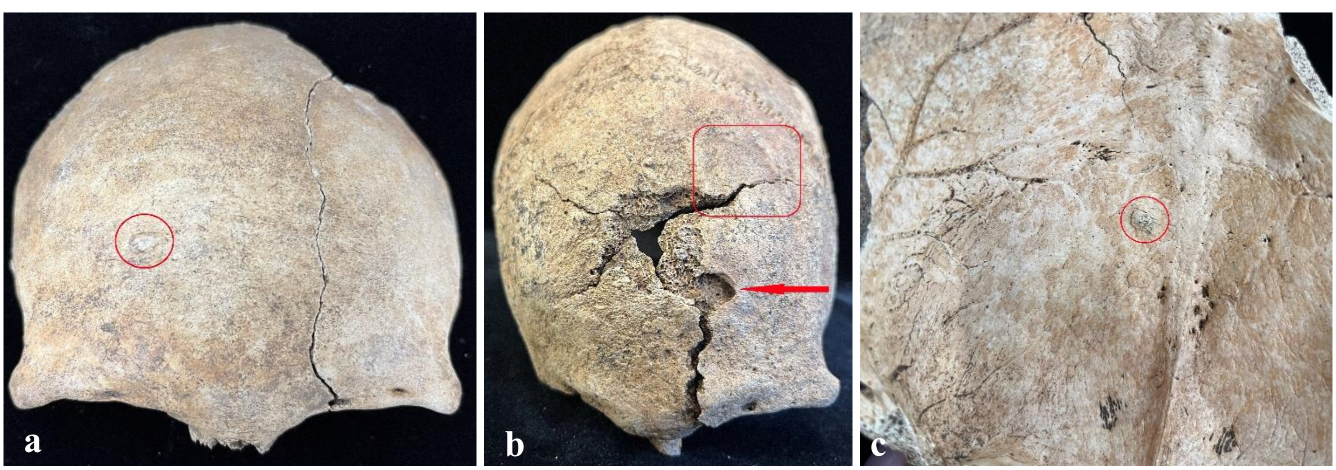

Figure 11. Possible cranial neoplastic lesions. SK2197 (I, 46+ years) (a), SK2529 (M, 17-25 years) (b), SK2516 (F, 46+ years) (c).

5.8 Circulatory disease

Disruptions in the circulatory system result in the fragmentation and collapse of skeletal joints. One such pathology is osteochondritis dissecans (OCD), which usually affects young males in the first decade of life. It is now commonly considered to be a traumatic lesion (Roberts et al. 2026, 113). Bone tissue death occurs following disruption to the blood supply in that area, either by normal processes or following chronic traumatic injury. Osteochondritis dissecans is usually 'well-defined, porous, often circular…' (Roberts and Manchester 1995, 89). Eight individuals (over the age of 10.6 years) displayed one or more erosive lesions consistent with OCD (Table 9) (n=8/30, CPR=26.7%).

Table 9. Individuals with osteochondritis dissecans

Skeleton number	Biological Sex	Age (years)	Region	Side	Location of lesion(s)
2199	Indeterminate	17-25	Scapula	Right	Glenoid cavity
2217	Female	46+	Scapula	Right	Glenoid cavity
			Clavicle	Right	
			Femur	Left	Distal, lateral condyle
2503	Female	26-35	C2 (axis)	Left	Superior articular facet
			Calcaneus	Right	Superior surface
2504	Female?	46+	Humerus (distal)	Right	Inferior surface of the trochlea
2511	Male	26-35	Radius	Bilateral	Tuberosity
2520	Male	18+	Tibiae	Bilateral	Distal joint surface (in angle with medial malleolus)
2524	Nonadult	10.6-14.5	Tibia	Left	Distal epiphysis
2537	Male	46+	Pedal proximal phalanx	?Left	Proximal end of the proximal phalanx of the ?left big toe

Another circulatory condition was evident in a 10.6-14.5 individual (SK2523) who had asymmetrical inferior foramina of the axis (or C2), with the right foramen larger than the left. The foramen is extending into the right superior articular facet (Figure 12). While asymmetrical foramina may be the result of normal variation, the presence of an erosive lesion with smooth, remodelled edges may suggest a pressure defect. Asymmetrical foramina of cervical vertebrae may be the result of two abnormalities of the vertebral artery: a tortuosity or an aneurysm (Antoine and Waldron 2023, Waldron and Antoine 2002). A tortuosity results if a segment of the vertebral artery becomes looped or coiled, causing an increase in pressure and pushing against the bone can cause the enlarged defect. In contrast, and aneurysm is a localized expansion (bulge) and thinning/weaking of the artery wall can also erode an adjacent bony structure (Antoine and Waldron 2023). In addition to tortuosity and aneurysm, differential diagnosis should also consider a neurofibroma (a benign nerve-sheath tumour). Clinical symptoms of tortuous loops may not cause any symptoms, however, if the cervical nerve roots are compressed, neurological symptoms and/or neck pain may result (Antoine and Waldron 2023). Aneurysms may lead to strokes, which may be identifiable as bony or muscular atrophy, which was not immediately identifiable in SK2523. While pressure defects caused by a tortuosity and an aneurysm are similar in bony characteristics, the lesion observed in the C2 of SK2523 is consistent with that published by Antoine and Waldon (2023, Figure 10.4, page 192), which the authors have diagnosed as more likely to be a tortuosity than an aneurysm.

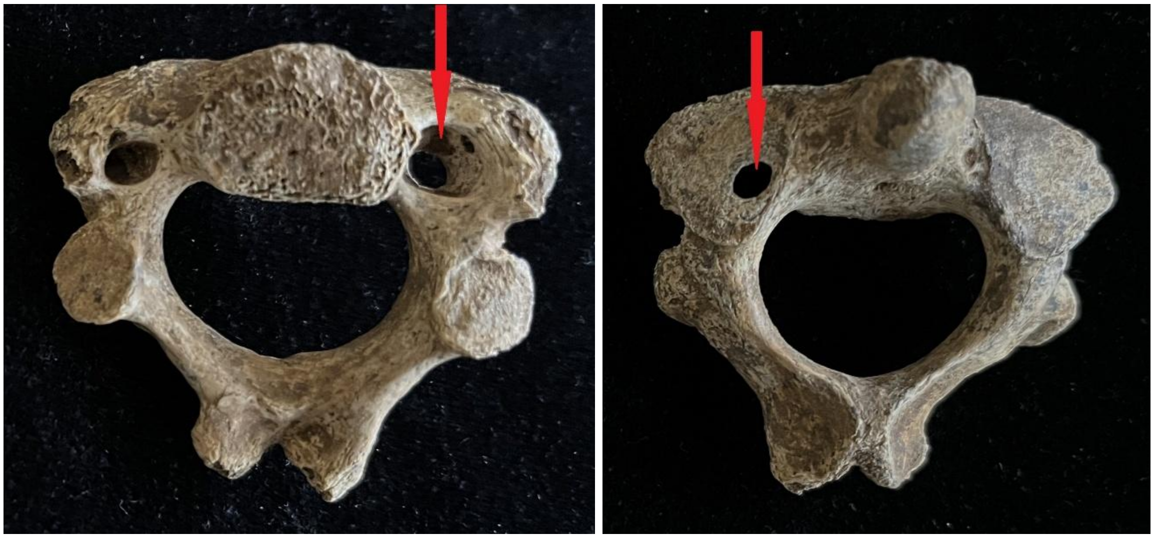

Figure 12. Possible tortuosity of the right foramen of the axis (C2) of SK2523.

5.9 Metabolic Disease
Metabolic diseases are a group of conditions caused by a deficiency of nutrients due to undernutrition, malnutrition, infection or abnormal processing of vitamins and minerals (Roberts et al. 2026). One individual, a 2.6-6.5 year old (SK2525), displayed evidence of possibly scurvy (CPR = 1/13 non-adults, 7.7%). Grey woven bone was evident on the greater wing of sphenoid, the alveolar processes of the maxilla and mandible, in addition to porosity on the endocranial surface of the basilar process. While porosity of the basilar process may be an indication of normal growth (Eggington et al. 2024), the combination of the other pathological alterations suggest scurvy as a possible cause.

5.10 Miscellaneous conditions
5.10.1 Hyperostosis frontalis interna
Two older females (n=2/14 females, CPR=14.3%), SK2505 and SK2515, displayed the characteristic morphological changes of the endocranial surface of the frontal bone for hyperostosis frontalis interna (HFI), including a striated appearance and raised nodule formation. Although the aetiology of HFI is still unknown, there is a strong relationship between age, biological sex and the presence and severity of HFI (i.e. women of advanced age appear to display the most severe expressions of HFI). It is thought to result from altered sex hormonal levels, as it most frequently affecting post-menopausal women (Buikstra 2019). This change in hormones results in the thickening of the cranial bones, and nodule formation on the endocranial surface, primarily of the frontal bone.

5.10.2 Arachnoid granulations
Also observed on the endocranial surface of the cranium were small, localised erosive lesions, characteristic of arachnoid granulations - small and well-defined depressions on the endocranial surface of the skull. They commonly form clusters on the parietal bones, or can be found on the frontal bone, and have been reported to increase in number with advancing age (Barber 1995), although this has been queried, as they have been found to occur at any age (Radoš et al. 2021). As summarised in Table 10, 14 adult individuals (n=14/25 adults with

cranial remains, CPR=56.0%). Further investigations of arachnoid granulations in these individuals should assess the number, location, and identify those lesions with increased vascularisation.

Table 10. Summary of individuals with arachnoid granulations (and other areas of porosity) on the endocranial surfaces of the cranial vault

Skeleton number	Biological sex	Age (years)	Description
2197	Indeterminate	46+	Arachnoid granulations, deep middle meningeal grooves, macroporosity on internal occipital protuberance
2501	Female	36-45	Arachnoid granulations
2502	Indeterminate	26-35	Nodules/spicules frontal, arachnoid granulations, temporal erosive lesions
2503	Female	26-35	Arachnoid granulations
2505	Female	46+	Arachnoid granulations, deep middle meningeal grooves, erosive lesions on sphenoid
2510	Male	46+	Arachnoid granulations
2511	Male	26-35	Arachnoid granulations – frontal/parietals
2512	Female?	46+	Arachnoid granulations
2516	Female	46+	Possible arachnoid granulations
2517	Male	46+	Arachnoid granulations
2529	Male	18-25	Arachnoid granulations or something else?
2530	Female	46+	Arachnoid granulations
2534	Female	46+	Arachnoid granulations
2537	Male	46+	Arachnoid granulations

5.10.3 Decubitus lesions (pressure sores)

Two females, SK2218 (26-35 years) and SK2504 (46+ years) displayed localised areas of porosity on the ischial tuberosities. The lesions were unilateral in each individual, with the right ischium affected in SK2218, and the left ischium in SK2504 (Figure 13ab). Although research for such lesions is in the early phases in the bioarchaeology community, it may be possible these lesions represent pressure sores (decubitus lesions), produced from being in one position for an extended period of time.

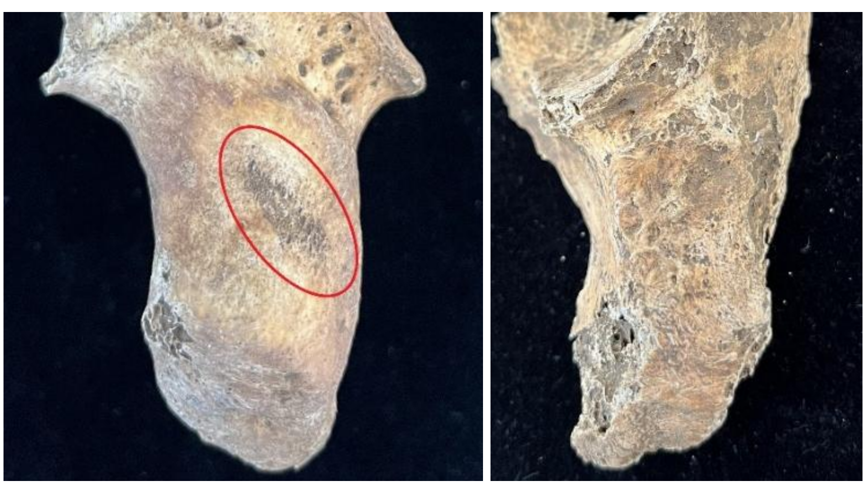

Figure 13. Erosive lesions (possible pressure sores) on the ischial tuberosities of SK2218 (a, circled), and SK2504 (b).

5.10.4 Miscellanea

During skeletal analysis, anomalies of the remains may be noted, which may be within the range of normal variation, or may be truly pathological. Although it is not always possible to identify the skeletal changes to a specific disease process, they warrant further investigation (Table 11).

Table 11. Summary of additional skeletal observations, which require further research for the 2024-5 burials.

Skeleton	Biological sex	Age (years)	Description
2197	Indeterminate	46+	Posterior foramina on C1, bone former (enthesophytes/spurring on most muscle attachments), deep middle meningeal grooves, macroporosity on internal occipital protuberance
2199	Indeterminate	17-25	Pronounced lateral bend to the distal humerus (healed rickets?)
2202	Male	46+	Frontal bone is very thick (thickened endocranial layer)
2217	Female	46+	All skeletal elements are notably porous
2218	Female	26-35	Porosity of the internal occipital protuberance, abnormal pinched appearance to the thoracic spinous processes, deep foramina inferior to the L5 superior articular facets, localised porosity on right ischium (superior tuberosity)
2500	Male	46+	Deep sulcus on right side of endocranial occipital, asymmetrical bodies of L4 and L5 (pinched towards the right side), large foramen/remodelling bone on left dorsal ilium, holes (taphonomic?) on right femur (distal/anterior), superior S1 (left side), right ilium (ventral), pronounced/spiculated tibial soleal lines (left more than right)
2501	Female	36-45	Ossification of ligamentum flavum throughout thoracic spine, lytic depressions to anterior/medial shaft of left distal femur
2502	Indeterminate	26-35	Nodules/spicules on endocranial frontal bone, erosive lesions to right temporal (endocranial surface, anterior to the petrous portion), pronounced humeral muscle attachments (proximal/anterior) and radial tuberosities, cortical defects of inferior/sternal claviculae
2503	Female	26-35	Arachnoid granulations/ erosive lesion endocranial frontal bone, deep grooves/depressions superior to acetabula and distal ulnar shafts, erosive defects on sternal claviculae and ischia, claviculae are very different curvatures, porous/striated vertebral bodies
2504	Female?	46+	Cranial vault fragments are thick and lightweight, erosive depressions on left ischium, right 2nd metacarpal (palmar) and right metatarsals, bowed curvature to the femoral shafts
2505	Female	46+	Deep etching of middle meningeal grooves (right side), erosive lesions on sphenoid,
2506	Female	46+	Broad nasal aperture, erosive lesions of left endocranial temporal bone (anterior) and sphenoid (posterior orbital surface), deep transverse sinus (occipital), diffuse porosity (right clavicle, rib shafts, thoracic vertebrae (spinous processes), ischia, strong muscle attachments (proximal humeri), oblong defects on proximal/lateral ulnae, radii are very curved, unusual shape to femoral heads and neck angles
2508	Indeterminate	10.6-14.5	Deep sulci at the base of the cranium, and deep meningeal grooves, depression on the endocranial surface of the frontal bone (to the right of the midline, superior to glabella), possible asymmetrical humeri, and unusual medial curvature to right proximal humerus
2510	Male??	46+	Asymmetric cranial vault (sagittal suture does not run down the midline)
2511	Male	26-35	Irregular (undulating) body surfaces (superior and inferior) of T11-L5
2512	Female?	46+	Gracile (small) elements, but strong muscle attachments (especially posterior/superior femora and inferior gluteal lines on posterior ilia), possible erosive lesions on metatarsals
2514	Male	26-35	Asymmetrical limbs, maxillary canines and molars have unusually short roots, cortical defects of right proximal/anterior humerus, erosive lesions on sphenoid, anterior tali, superior calcanei and naviculars, posterior S1 body
2515	Female	46+	Depression/porosities on left side of sella turcica, with possible remodelling on inferior surface, pronounced tuberosity on left navicular medial tuberosity
2516	Female	46+	Nodule of new bone (light-coloured, porous, woven bone) left of the midline of the endocranial frontal bone (not classic HFI), thickened cranial vault, rugged surface with ?arachnoid granulations. Erosive lesions on sphenoid.

Skeleton	Biological sex	Age (years)	Description
2517	Male	46+	Arachnoid granulations and increased parietal porosity, medial-lateral bowed left femur
2519	Indeterminate	2.6-6.5	Very deep transverse sinus impressions on the endocranial temporals, superior/medial surfaces of the petrous portions, and partes laterales (right side is much deeper than the left), possible erosive lesions along the midline of the endocranial surface of the frontal bone, and greater wings of sphenoid, large foramina on anterior ilia, lateral bending of distal femora (possible rickets/scurvy?)
2520	Male	18+	Deep depressions on palmar surface of proximal phalanges (distal ends), femora are very broad/flat (L>R), possible erosive lesion on left anterio-medial patella, spurring of proximal patellae and posterior calcanei, bony projections on plantar calcanei
2521	Male	46+	Cortical defects of inferior/sternal claviculae, much ligament ossification of thoracic vertebrae
2522	N/A	6.6-10.5	Depressions on endocranial occipital bone (internal occipital protuberance) and superior surfaces of greater wings of sphenoid, raised projections on right distal humerus shaft (anterior), abnormal torsion of left femur. Further analysis needed for possible rounded blunt force trauma to forehead (midline) and possible lesion to right femur (proximal/posterior/medial)
2523	N/A	10.6-14.5	Asymmetrical frontal bone and humeri, possible scaphocephaly, cortical defects of inferior sternal claviculae, depression of superior right rib 1, pronounced nutrient foramen (?) anterior sternal body, irregular topography of lumbar bodies (superior and inferior), cribra femoralis (bilateral), ovoid trabecular depression of left proximal/ posterior tibial shaft
2524	N/A	10.6-14.5	Cortical defects of musculature on the anterior surfaces of the proximal humeral shafts, trabecular bone in coronoid fossa of the right distal humerus, bilateral cribra femoralis
2526	N/A	2.6-6.5	??Abnormal frontal bone (left orbit seems too high to the articulation for the nasal bones?), abnormal depressions on endocranial surface of left occipital bone
2529	Male	17-25	Non-fusion of the left sphenoid and frontal bone (squamous-like suture, ?non-metric trait?), cranial vault is quite arched in the midline at the mid-parietal area, depressions along sagittal suture (?arachnoid granulations or something else), porosity of superior petrous portions, asymmetrical robusticity of humeri, grooves etched into the posterior left ilium (vascular or taphonomy?)
2530	Female	46+	Sharp anterior projections of proximal humeral musculature, possible erosive lesions on carpals and tarsals
2534	Female?	46+	Arachnoid granulations (frontal and parietals), roughened endocranial frontal bone, “scales” anterior to left TMJ, deep transverse sinus on right temporal bone with erosive lesions on the floor of the sinus, porosity over right orbit, cortical defects on right inferior/sternal clavicle, radial tuberosities and proximal/anterior ulnae, possible large, circular erosive lesion on medial surface of left distal radius, erosive lesions on right trapezium and trapezoid, right talus and calcaneus, small lump of bone on medial 1/3 of right femoral shaft, symmetrical holes on dorsal cuboids, MT1s and left navicular, cribra femoralis(?) right anterior femur, possible erosive lesions on superior/lateral S1 body, buttressing of posterior ilia, left posterior/medial ilium is striated, iliac crest osteophytes
2536	N/A	6.6-10.5	Hypervascularisation impressions on the endocranial surface of the cranial vault (possible active bone remodelling), raised lump on proximal shaft of posterior left femur
2537	Male	46+	Large porosities on orbit roofs, erosive lesions (?) on superior temporals petrous portions, remodelled bone on the sphenoid, guttering/remodelling of the nasal aperture, smooth facet along left superior scapular spine, abnormal morphology of superior edges or ribs (?musculature)

6.0 Discussion

6.1. Demography

This report has detailed the demographic and pathological alterations of the 40 skeletons excavated in the 2024 and 2025 field seasons. Combining the osteological results for 2022-3 (Falys 2025) and that detailed here (2024-5), this brings the total number of single inhumations to 63 for the COP22-25 excavations (i.e., does not include assessment of any disarticulated human bone). Overall, there are nearly equivalent numbers of adult females (n=23, 36.5%) and males (n=20, 31.7%) and the trend for mature adults (46+) continues. The 2025 season yielded many more children than previous excavations (n=13) and perhaps because excavations were concentrated on a new area of the cemetery. Further excavation of the north-west quadrant of Trench 2 is needed to explore whether this area is, perhaps, the preferential place of burial for non-adult individuals within the larger cemetery landscape, or were discovered due the shallow nature of the burials. Excavation into the lower layers of soil may or may not identify further adult/non-adult burials interred beneath. The current demographic profile of the site is presented in Figure 14.

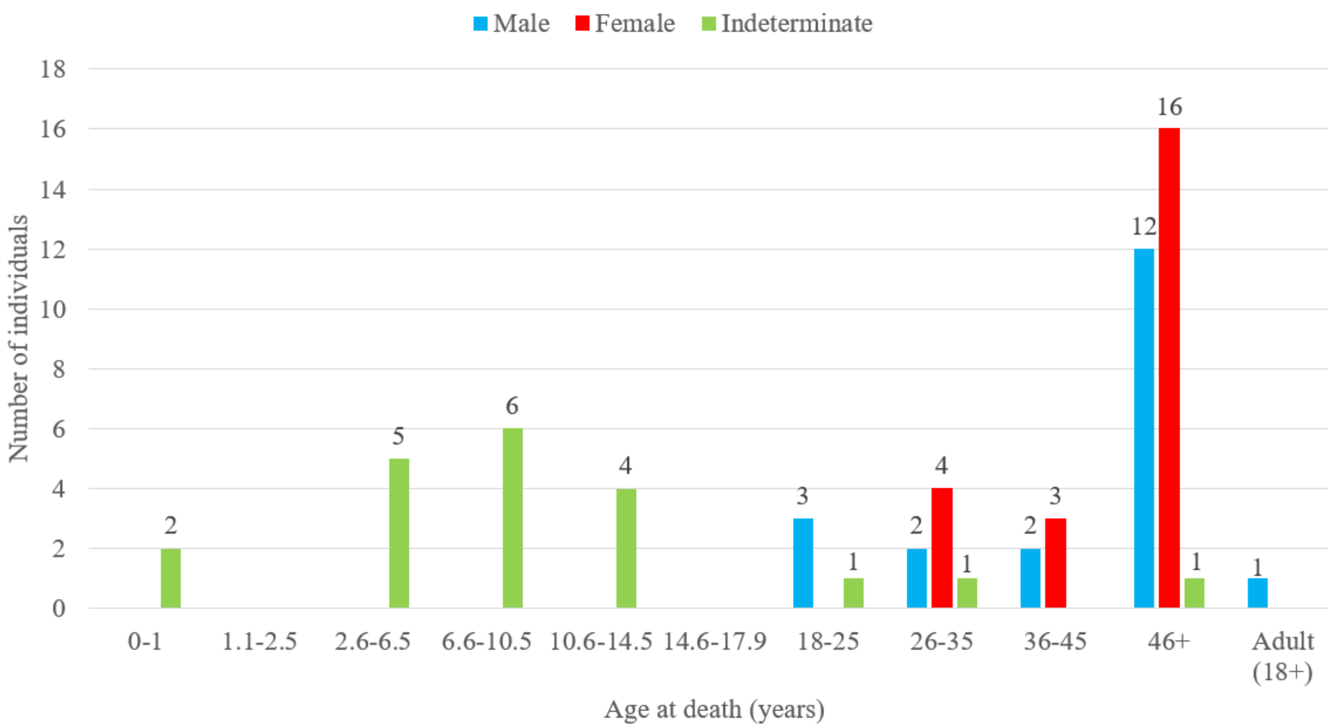

Figure 14. Demography of the combined sample (n=63).

The further excavation of the cemetery during 2024-5 confirmed the burials in all areas of Trench 2 are well organized in a series of rows that run approximately north-south and east-west. The density of burials is much higher in the western side of Trench 2, with markedly more disturbance of underlying graves (and subsequent re-use of the skeletal elements). Internments towards the middle of Trench 2 also show a higher degree of disarticulated human bone within the graves than was observed in the eastern-most burials during the 2023 field season.

The organized rows of burials within the eastern side of Trench 2, suggests the use of grave markers or other ways to identify where burials have been interred, although overtime these markers either disappeared, or the markers were not taken into consideration for later burials, leading to truncation and disturbance of the earlier graves. For example, a minimum of three intercutting burials were excavated at the southern end of Trench 2: SK2520, SK2521 and SK2500 (Figure 15a-d). SK2520 was interred first (i.e., the oldest burial), followed at a later date by SK2521, which truncated (and removed) the upper body of SK2520 (Figure 15a,b). SK2500 was the final burial in this area (i.e., the newest burial), overlying SK2521. At the time of excavation, it was noted the vertebral bodies of SK2521 were absent. It is likely the upper body of SK2521 was exposed while digging the grave for SK2500, ultimately damaging the anterior spine. Care was then taken to adjust the grave depth to ensure SK2521 was not damaged further, and SK2500 was interred.

Figure 15. Multiphases of burial at the southern end of Trench 2. First burial was SK2520 (a, legs only), second burial was SK2521 (b, was nearly complete), and last burial was 2500 (c), grave locations highlighted by red box (d).

Currently, there is no evidence that specific areas of the cemetery were reserved for specific age of sex groups (Figure 16).

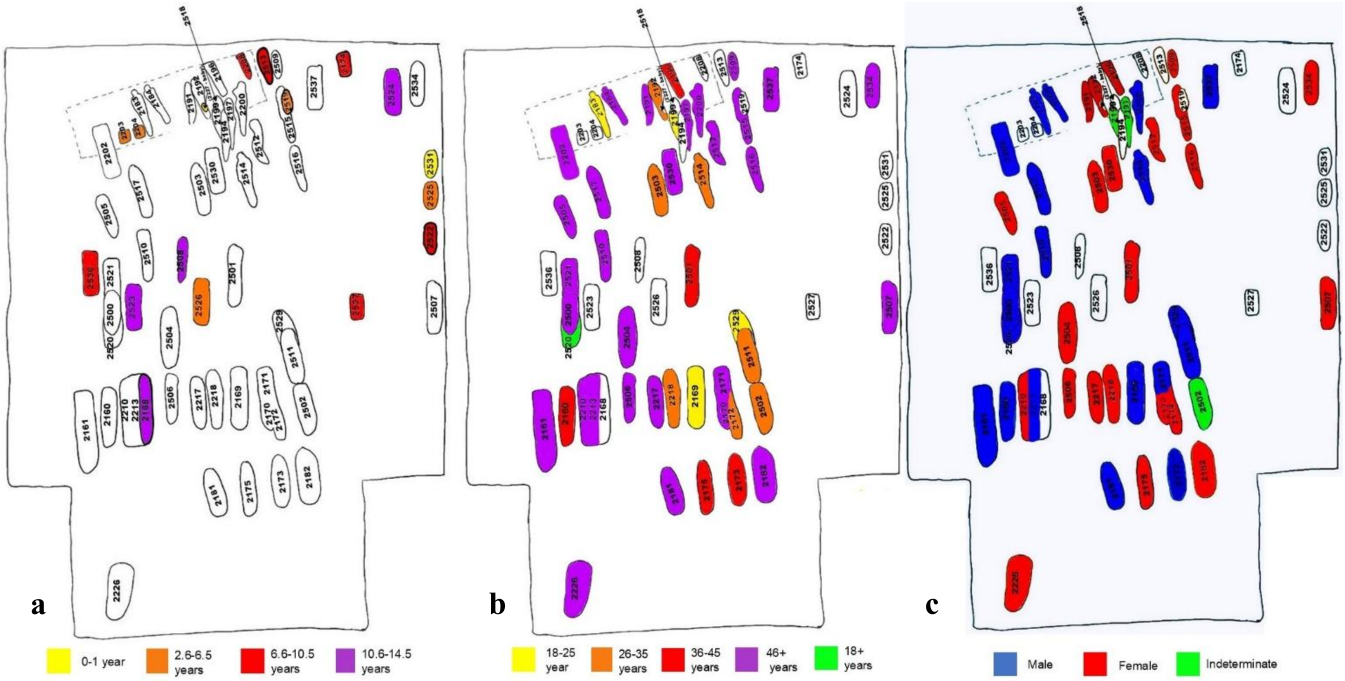

Figure 16. Burial location with respect to age-at-death – non-adults (a), adults (b), biological sex (c).

6.2 Stature

Additional stature estimates were provided by 19 individuals of the 2024-5 season individuals (8 males and 11 females, Figure 17). When combined with the 2022-3 figures, a total of 37 individuals were assessed for stature, ultimately providing a mean female stature of 159.5cm and a mean male stature of 173.1cm (Table 12).

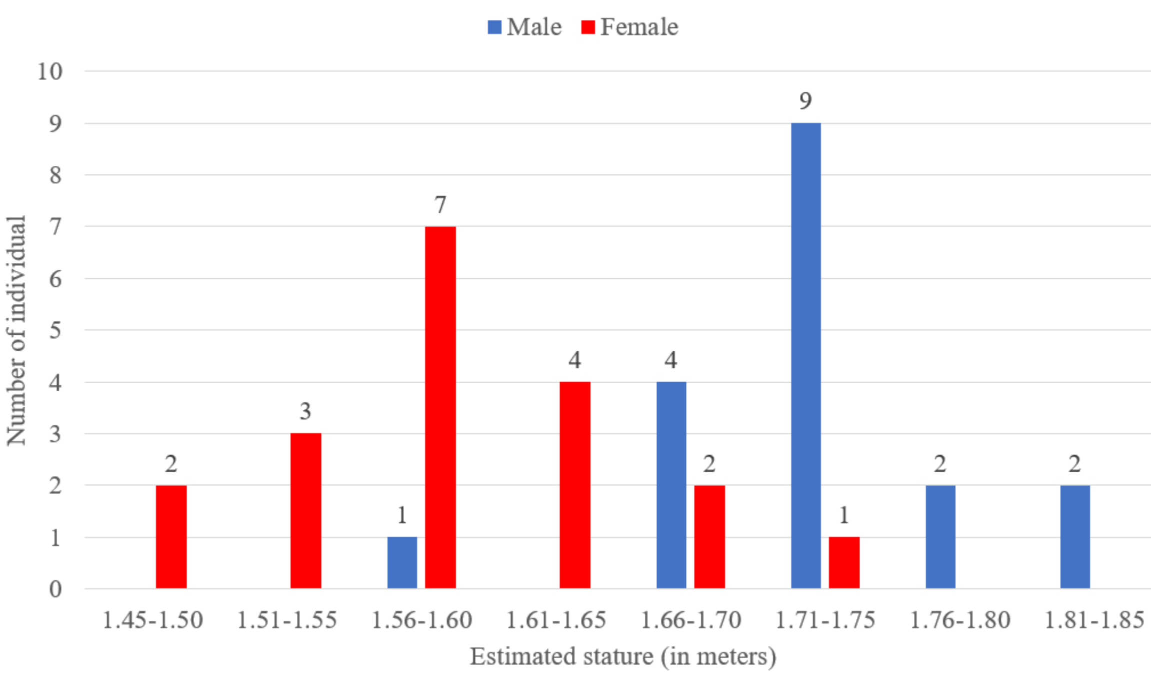

Figure 17. Stature estimates for the combined Cookham sample

The Cookham males are nearly 1cm taller than the average male stature for the period, and the females 1.5cm shorter (Roberts and Cox 2003). When compared to the individuals from two contemporaneous cemeteries, the Cookham males were taller than those from Staunch Meadow, but shorter than those buried at Nazingbury. The Cookham females were the shortest of all compared sites.

Table 12: Comparisons of statures (cm) with sites of similar date

Site	Males			Females		
	n	**Mean**	**Range**	**n**	**Mean**	**Range**
Cookham (combined)	**18**	**173.3**	**160.2-182.3**	**19**	**159.6**	**150.4-172.4**
[1]Staunch Meadow, Suffolk	25	171.8	160.1-186.5	14	159.9	147.8-175.2
[2]Nazingbury, Essex	10	175.3	170.0 -181.0	13	168.2	158.5-174.0
Roberts and Cox (2003)	996	172	170.0-182.0	751	161	152.0-170.0

[1]Tester et al. (2014); [2]Huggins (1978)

That the Cookham females are on average, shorter than their peers from other sites of the time suggests they experienced chronic poor health, combined with a mixture of other skeletal indicators of non-specific stress (enamel hypoplasia, asymmetric long bones) that impacted their childhood growth. As suggested in Falys (2025), future research could explore the age at menarche in the group (early menarche can affect final stature) and further explore growth and development by analysing vertebral canal size (VNC).

7. Health Status

By necessity, skeletal reports on pathological analysis break down observed lesions into distinct categories (e.g., trauma, degenerative joint disease, infection). By separating each pathology in this way, in order to assess the prevalence of a specific disease category within the population as a whole, we may miss the individual life story a single skeleton has to tell. The human body can, and does, experience more than one disease or stress event throughout life, which can either accumulate over time, and may occur concurrently. As with the individuals reported in from the 2022-3 excavations, many of the skeletons from the 2024-5 season experienced a series of health events that can tell us about their childhood environment, occupation, risk of injury, genetic predispositions and diet. These can be best illustrated through the construction of individual osteobiography as a powerful way to understand the lived experiences of the people interred at Cookham Abbey. A combined summary of the pathology from the 2022 to the 2025 excavations is provided in Appendix 2. This evidence continues to support five general health trends at Cookham Abbey, as highlighted in Falys (2025).

7.1 Advancing age

The majority of individuals buried within the portion of cemetery exposed by Trench 2 were of advanced age (traditionally described in bioarchaeology as over 46 years). The combined sample has almost equal numbers of adult females (n=23, 36.5%) and males (n=20, 31.7%), and 46.0% of the sample are over 46+ years (n=29, 12 males, 16 females, 1 indeterminate sex). This age demographic has contributed to the high prevalence of joint and diseases seen in the group. Of the 46 adult individuals, 81.5% had evidence of spinal or extra-spinal joint disease, and 22.2% suffered from osteoarthritis. The dentition displayed increasingly severe dental wear with age, ultimately predisposing teeth to caries (CPR=32.7%), as well as the accumulation of calculus (plaque) (CPR=63.3%) and periodontal disease (CPR=78.6%), all contributing to the loss of permanent teeth or AMTL (CPR=53.5%, TPR=11.7). Futher research on this group will allow the older Cookham individuals to be further separated into the “young-old” (46-70 years) and “old-old” (e.g., 70+ years) using methods developed by Falys (2012) and Milner et al. (2026 -Transition Analysis 3), to explore issues of frailty and advancing age.

7.2 Habitual strenuous activity

Evidence for strenuous activity in the day to day lives of these individuals is evidenced by the prevalence of lesions in the spine in both sexes, indicative of bending and lifting activities from a relatively young age (Schmorl’s nodes, CPR=34.8%). Occupational stress is also seen in the form of osteochondritis dissecans (OCD), resulting in localised bone death due to repetitive trauma (CPR= 32.7%). The presence of spondylolysis (in the spine, CPR=8.3%) and os acromiale (in the shoulder, CPR=2.0%), while they may also have underlying genetic predisposition, hint at repetitive strenuous activity in the lives of the people at Cookham. The activities being undertaken were seemingly hazardous, as indicated by the observed prevalence of antemortem trauma (CPR=65.2% of adults).

7.3 Exposure to environmental stress

Before the discovery of antibiotics, childhood infections and periods of malnutrition would have been common. These stressors are recorded in skeletal remains in the form of sub-periosteal new bone formation, defects in the forming enamel (hypoplasia), and porous lesions in the orbits (cribra orbitalia). The prevalence of enamel hypoplasia and sub-periosteal new bone were found to be 60.4% and 68.3%, respectively. The latter identifies that over two-thirds of Cookham individuals displayed areas of active or healing periosteal reaction when they died, this may be indicative of physiological stress or active disease in the months prior to death, but further investigation is needed to map out the location of these lesions to see if any patterns emerge.

Enamel hypoplasia provide information on recovery from childhood stress, as they cannot form once the teeth have completed development in adulthood. Nearly two-thirds of the individuals, displaying linear defects, experienced malnutrition or disease before the age of 7 years. The short stature, primarily of the females at Cookham, as well as asymmetry of the bones of the arm (humerus) and leg (femur) in some individuals may also have resulted periods of stress in their early years. As highlighted in Falys (2025), further work on additional stress indicators such as vertebral neural canal size (VNC) will further elucidate the impact of childhood living conditions on the lifelong health of these individuals.

7.4 Chronic and debilitating conditions

The Falys (2025) report identified a high prevalence of individuals with chronic pathological conditions, with many suffering some a health challenge that would have been obvious to those in their community. The 2024-5 season has revealed increasing evidence for debilitating trauma in the group (CPR=65.2%), with some fractures in the process of healing, and others that had clearly not been medically treated, either by reducing the fracture (i.e., pulling the two ends back into alignment), or being splinted leaving the limbs them severely misaligned or shortened. Future research should focus on the prevalence of antemortem trauma during this period, both in monastic and lay cemeteries, to identify the normal baseline for healed trauma in the 7^{th}-9^{th} centuries in order to ascertain whether the extent of trauma at Cookham is exceptional.

The consequence of not treating fractures was subsequent physical challenges for the individuals. For example, the atrophy of the left humerus of SK2202 indicated the left arm was likely not used for many tasks following fractures of the left forearm. In some cases, hip problems that would have produced physical limitations were evident in the body position of the individual within the grave, likely inhibiting the positioning the body in the correct way for the Christian burial rite (i.e., supine and extended). For example, following the fracture of her right hip and subsequent healing in an abnormal position, one female (SK2530) would have had a limited range of motion, as indicated by the semiflexed position of her right leg in the burial (Figure 18). Although it is not possible to identify the underlying cause skeletally, two other females (SK2510 and SK2512) also had semiflexed legs likely the result of underlying physical limitation in life.

Figure 18. Hip pathology and burial position. SK2530 (a), SK2510 (b), SK2512 (c).

Other chronic conditions were identified during the 2024/25 field seasons, including tuberculosis and possible scurvy in the children, as well as possible neoplastic disease in adults. Further research is needed for several individuals in order to understand the causes of the observed skeletal alterations.

7.5 Treatment and care

Two further individuals displayed erosive lesion on the ischial tuberosities (in the inferior pelvis) in which may represent pressure sores. Their presence suggest individuals were sat/laying down for extended periods of time, during which "bed sores" developed to such an extent that they reached the bone. A further four individuals had thin layers of occlusal calculus in the wear facets of the teeth, which, for whatever reason (e.g., pain while chewing, paralysis) suggests the affected individuals were not able to actively chew food on one or both sides of their mouths for weeks or months leading up to their deaths. Future research could employ the "index of care" (Tilley 2012, 2015; Tilley and Schrenk, 2017), in order to assess which individuals would have required help from others in their communities to live with their health conditions or physical disabilities.

The addition of data from 2024-25 adds to the evidence that the majority of interred individuals either had physical struggles during life (i.e., signified by antemortem trauma), poor health leading up to their deaths (i.e. sub-periosteal new bone formation/specific infection), or suffered from the aches and pains of a long-lived active life (i.e., old age). It is only with the comparison of demographic and pathological data with extensive further research of contemporaneous skeletal populations of differing settlement type (i.e., monastic, rural and urban communities) that a case may be made whether it is a possibility that individuals coming to Cookham Abbey in search of healing or hospice care, or whether they were buried at Cookham Abbey in a location designated for those who were perhaps physically distinctive, or 'other' from their peers (Hadley 2010).

As an additional osteological update, samples for aDNA were taken in August 2025, and are currently being analysed at the Crick Institute, London. It is hoped the results will provide information confirming biological sex, and provide information for ancestry, familial relationships, and (hopefully) viral infection.

8. Future Research

The palaeopathological observations from this portion of the Cookham Abbey cemetery has highlighted the need for extensive future research, which should include:

1) Radiographs and further research into the cases of possible antemortem trauma, neoplastic disease, undiagnosed erosive lesions and unusual morphologies of skeletal elements in the 2024-5 individuals.
2) Preliminary analyses did not investigate the "index of care" (i.e., needs of the individuals), frailty index, non-metric traits, or observed unusual dental wear patterns in all 2022-25 individuals
3) Stable isotope analysis (C/N) to investigate diet, and chemical analysis of calculus deposits with the aim (or possibility) of identifying herbal medicines that may have been used. What insights can be made between the chemical results and writings of the Leech book, and for Anglo-Saxon medicine
4) Stable isotope analysis (Sr/O) to investigate migration.
5) Explore the older individuals (i.e., 46+ years) following criteria by Falys (2012) and Transition Analysis 3, with the aim of separating the 29 2022-25 individuals of advanced age into those aged approximately 46-70 years and 70+ years.
6) Produce osteobiographies for the individuals to fully understand the life stories written in their skeletons.
7) Re-analysis of contemporary early medieval skeletal populations to make data directly comparable in order to assess health, care, treatment, and burial rite in monastic (and non-monastic) communities in early medieval England.

Acknowledgements

Special thanks to the Friends of Cookham Abbey for funding this research, the staff and students of the Department of Archaeology at the University of Reading for their careful excavation and post-excavation processing of the skeletons, and Mary Lewis (University of Reading) for being my "phone a friend" for second opinions of pathological observations, and her ongoing support.

References Cited

AlQahtani, SJ, Hector, MP, Liversidge, HM, 2010, Brief Communication: the London atlas of human tooth development and eruption. *Am J Phys Anthrop* 142, 481-490

Aufderheide, A C and Rodríguez-Martín, C, 1998, *The Cambridge Encyclopedia of Human Paleopathology*, Cambridge

Antoine, D and Waldron, T, 2023, Abnormalities of the vertebral artery: are cervical pressure defects being overlooked in palaeopathology? In: Binder, M, Robers, CA, and Antoine, D, *The Bioarchaeology of Cardiovascular Disease*, Cambridge University Press, Cambridge, 174-201

Barnes, E, 1994, *Developmental Defects of the Axial Skeleton in Paleopathology*, Denver, Colorado

Berry, A C and Berry, R J, 1967, 'Epigenetic variation in the human cranium'. *Journal of Anatomy*, 101:361-379

Brickley, M and McKinley, J (eds), 2004, *Guidelines to the Standards for Recording Human Remains*, IFA Paper 7, Reading

Brooks, S T and Suchey, J M, 1990, 'Skeletal age determination based on the Os Pubis: a comparison of the Acsadi-Nemeskeri and Suchey-Brooks methods', Human Evolution, 5, 227–38

Brothwell, D R, 1981, *Digging up Bones: The Excavation, Treatment and Study of Human Skeletal Remains,* 3rd edn, Oxford

Buikstra, J E (ed), 2020, Ortner's Identification of Pathological Conditions in Human Skeletal Remains (3rd edition), Academic Press, London.

Buikstra, J E and Ubelaker, D H, 1994*, Standards for Data Collection from Human Skeletal Remains*, Arkansas Archaeological Survey Research Series, 44, Fayetteville, Ark

Cunha, E and Pinheiro, J, 2009, 'Antemortem trauma', in S Blaus and D H Ubelaker (eds), *Handbook of Forensic Anthropology and Archaeology,* Walnut Creek, Calif, 246–83

Cunningham, C, Scheuer, L, and Black, S, 2016, *Developmental Juvenile Osteology*, Academic Press, Oxford

Dias, G. and Tayles, N., 1997. 'Abscess cavity'—a misnomer. *International Journal of Osteoarchaeology*, *7*(5), pp.548-554.

Eggington, J, Pitt, R, and Hodson, C, 2024, A macroscopic assessment of porosity and new bone formation on the inferior *pars basilaris*: Normal growth or an indicator of scurvy? International Journal of Paleopathology 45:62-72

Falys, C G, 2012, 'Extending the Life Course: Developing new methods for identifying the "elderly" in the archaeological record', unpubl PhD thesis, Univ Reading

Falys, C, 2025, “The People of the Abbey” Skeletal analysis of inhumations from the 2022 and 2023 field seasons. Unpublished report

Falys, C G and Lewis, M E, 2011, ‘Proposing a way forward: A review of standardisation in the use of age categories and ageing techniques’, *Internat J Osteoarchaeology* **21(6)**, 704–16

Falys, C G and Prangle, D, 2015, ‘Estimating age of mature adults from the degeneration of the sternal end of the clavicle’, *American J Physical Anthropol* **156(2)**, 203–14

Falys, C G, Schutkowski, H, Weston, D, 2005, ‘The distal humerus--a blind test of Rogers' sexing technique using a documented skeletal collection’, *J Forensic Sciences* 50(6), 1289-93

Finnegan, M, 1978, ‘Non-metric variation of the infracranial skeleton’, *Journal of Anatomy*, 125:23-37

Hadley, D.M., 2010. Burying the socially and physically distinctive in later Anglo-Saxon England. *Burial in Later Anglo-Saxon England c*, *650*, pp.103-115.

Huggins, P J, 1978, Excavation of Belgic and Romano-British Farm with Middle Saxon Cemetery and Churches at Nazeingbury, Essex, 1975-6, Essex Archaeology and History, 10:29-117

Kyere, K, Than, K, Wang, A, et al. 2012, ‘Schmorl’s nodes’, *Eur Spine J* **21**, 2115–21

Langsjoen, O, 1998, ‘Diseases of the dentition’, in A C Aufderheide and C Rodriguez-Martin, *The Cambridge Encyclopedia of Human Paleopathology*, Cambridge, 393–412

Lewis, M E, 2018, *Paleopathology of Children*, London

Lovejoy, C O, Meindl, R S, Pryzbeck, T R and Mensforth, R P, 1985, ‘Chronological metamorphosis of the auricular surface of the ilium: A new method for the determination of adult skeletal age at death’, *American J Physical Anthropol* **68**, 15–28

McKinley, J, 2004, ‘Compiling a skeletal inventory: disarticulated and co-mingled remains’. In Brickley, M and McKinley, J (eds), *Guidelines to the Standards for Recording Human Remains*, IFA Paper 7, Reading, p 16

Milner, GR, Getz, SM, Weise, S, Tarp, P, Ousley, SD, Boldsen, JL, *in press*, Transition analysis 3: New skeletal age indicators. *Forensic Science International*.

Mitchell, P. D., & Brickley, M (eds), 2017, *Updated Guidelines to the Standards for Recording Human Remains.* Chartered Institute for Archaeologists/British Association for Biological Anthropology and Osteoarchaeology, Reading.

Radoš M, Živko M, Periša A, Orešković D and Klarica M, 2021, ‘No arachnoid granulations—no problems: number, size, and distribution of arachnoid granulations from Birth to 80 Years of Age’, *Frontiers in Aging Neurosci* 13:698865

Roberts, C and Cox, M, 2003, *Health and Disease in Britain: From Prehistory to the Present Day,* Stroud

Roberts, CA, Lewis, ME, Duffin, J, and Manchester, K, 2026, The Archaeology of Disease (4th edn). Cornell University Press, London

Roberts, C A, 2009, *Human Remains in Archaeology: A Handbook,* CBA Practical Handbooks in Archaeology, **19**, York

Rogers, T L, 1999, 'A visual method of determining the sex of skeletal remains using the distal humerus', *J Forensic Sciences* **44**, 57–60

Schatz, R, 2021, 'Cribriotic lesions in archaeological human skeletal remains. Prevalence, co-occurrence, and association in medieval and early modern Netherlands', *International Journal of Paleopathology*, 35:81-89

Lewis, M, and Falys, 2020, 'Puberty in the Past', *The Archaeologist*, 109:10-11

Lewis, M, Shapland, F and Watts, R, 2016, On the threshold of adulthood: a new approach for the use of maturation indicators to assess puberty in adolescents from medieval England, American Journal of Human Biology, 28(1):48-56

Stewart, TD, 1979, *Essentials of Forensic Anthropology*, Springfield Illinois, C.C. Thomas

Tester, A, Anderson, S, Riddler, I and Carr, R, 2014, *Staunch Meadow, Brandon, Suffolk: a high status Middle Saxon settlement on the fen edge*. East Anglian Archaeology Report No. 151

Tilley, L, 2012, 'The bioarchaeology of care', *The SAA Archaeol Rec* 12:3, 39–41

Tilley, L, 2015, *The Theory and Practice in the Bioarchaeology of Care*, Cham: Springer

Tilley, L, and Schrenk, A (eds), 2017, *New Developments in the Bioarchaeology of Care: Further Case Studies and Expanded Theory*, Cham: Springer

Trotter, M, 1970, Estimation of stature from intact long bones. In: TD Stewart (ed.) *Personal identification in Mass Disasters* pp. 71-83, Washington DC, Smithsonian Institution Press

Tyrell, AJ, 2000, Skeletal non-metric traits and the assessment of inter- and intra-population diversity: Past problems and future potential. In Cox, M and Mays, S (eds) *Human Osteology in Archaeology and Forensic Science*. London:Greenwich Medical Media.

Waldron, T and Rogers, J, 1991, 'Inter-observer variation in the coding osteoarthritis in human skeletal remains', *Internat J Osteoarchaeology* **1,** 49–56

Waldron, T and Antoine, D, 2002, Tortuosity or aneurysm? The paleopathology of some abnormalities of the vertebral artery. *Internat J Osteoarchaeology* **12**:79-88

Walker, P L, Bathurst, R R, Richman, R, Gjerdrum, T and Andrushko, V A, 2009, ‘The causes of porotic hyperostosis and cribra orbitalia: A reappraisal of the iron-deficiency-anemia hypothesis’, *American J Physical Anthropol* **139**, 109–25

Zelazny KG, Sylvester AD, Ruff CB, 2021,‘Bilateral asymmetry and developmental plasticity of the humerus in modern humans’. *American Journal of Physical Anthropology* **174**: 418–433

APPENDICES

APPENDIX 1: Summary of the observed pathological conditions of the Cookham 2024/25 individuals

Skeleton	Biological sex	Age (years)	Congenital	Metabol./ endocrine	Non-spec. stress	Infection		Joint Disease			Circ	Neopl	Trauma		Care?		
						Non Specif	Specif	DJD	OA	SN			Ante	Peri	Occl Calc	Decub	Surg
2197	Ind.	46+			Yes			Yes				Yes					
2199	Ind.	17-25		Poss	Yes	Yes					Poss						
2202	Male	46+			Yes			Yes	Yes				Yes				
2203	n/a	2.6-6.5			Yes												
2204	n/a	2.6-6.5			Yes	Poss											
2217	Female	46+			Yes	Yes		Yes			Yes						
2218	Female	26-35	Yes					Yes					Yes			Yes	
2500	Male	46+	Yes		Yes	Yes		Yes					Yes				
2501	Female	36-45			Yes	Yes		Yes				Poss	Yes				
2502	Ind.	26-35	Possible		Yes			Yes				Yes			Yes		
2503	Female	26-35	Yes		Yes	Yes		Yes			Yes				Yes		
2504	Female?	46+						Yes			Yes		Yes			Yes	
2505	Female	46+		Yes		Yes		Yes	Yes			Poss					
2506	Female	46+				Yes		Yes	Yes				Poss		Yes		
2507	Female	46+						Yes							Yes		
2508	n/a	10.6-14.5			Yes												
2509	Female	46+				Poss		Yes									
2510	Male??	46+				Yes		Yes									
2511	Male	26-35	Possible		Yes	Yes		Yes			Yes		Yes				
2512	Female?	46+				Yes		Yes					Poss				
2513	N/A	6.6-10.5			Yes								Yes				
2514	Male	26-35			Yes	Yes		Yes					Yes				
2515	Female	46+		Yes		Yes		Yes				Poss	Poss				
2516	Female	46+			Yes	Yes		Yes					Yes		Yes		
2517	Male	46+						Yes	Yes				Yes				

Skeleton	Biological sex	Age (years)	Congenital	Metabol./ endocrine	Non-spec. stress	Infection		Joint Disease			Circ	Neopl	Trauma		Care?		
						Non Specif	Specif	DJD	OA	SN			Ante	Peri	Occl Calc	Decub	Surg
2519	N/A	2.6-6.5		Possible	Yes												
2520	Male	18+				Yes		Yes			Yes						
2521	Male	46+						Yes	Yes				Yes				
2522	N/A	6.6-10.5					Poss										
2523	N/A	10.6-14.5	Yes			Yes					Poss		Yes				
2524	N/A	10.6-14.5				Yes					Yes	Poss					
2525	N/A	2.6-6.5		Possible													
2526	N/A	2.6-6.5				Yes								Poss			
2527	N/A	6.6-10.5			Yes		Yes										
2529	Male	17-25				Yes						Poss					
2530	Female	46+				Yes		Yes	Yes			Poss	Yes				
2531	N/A	0-1				Poss											
2534	Female?	46+						Yes	Yes	Yes							
2536	N/A	6.6-10.5			Poss	Poss											
2537	Male	46+				Yes		Yes	Yes		Yes		Yes	Poss			

APPENDIX 2: Crude prevalence rates of identified pathologies for the combined 2022-25 burials. * = requires further research

Condition	**2024-2025**			**2022-2023** (Falys 2025)			**Combined 2022-2025**		
	n	**Affected**	**CPR (%)**	**n**	**Affected**	**CPR (%)**	**n**	**Affected**	**CPR (%)**
Dental									
AMTL	24	16	66.7 (TPR 10.7)	19	7	36.8 (TPR 11.6)	43	23	53.5 (TPR11.7)
Caries	36	8	22.2 (TPR 3.0)	19	10	52.6 (TPR 4.2)	55	18	32.7 (TPR 3.6)
Calculus	36	17	47.2	19	18	94.7	55	35	63.3
Occlusal calculus	36	5	13.9	19	7	36.8	55	12	21.8
Periapical lesions	36	2	5.6	20	4	20.0	56	6	10.7
Periodontal disease	23	20	87.0	19	13	68.4	42	33	78.6
Enamel hypoplasia	34	20	58.8	19	12	63.2	53	32	60.4
Congenital / Developmental									
Lumbarisation	30	2	6.7	18	5	27.8	48	7	14.6
Spina bifida occulta	30	1	3.3	19	7	36.8	49	8	16.3
Spondylolysis	30	2	6.7	18	2	11.1	48	4	8.3
Os acromiale	29	0	0	19	1	5.3	48	1	2.0
Trauma*									
Antemortem	*27*	*19* adults*	*70.4*	*19*	*11* adults*	*57.9*	*46*	*30**	*65.2 (adults)*
Perimortem	*40*	*2**	*5.0*	23	1	4.3	*63*	*3**	*4.8*
Joint Disease									
DJD	27	22	81.5	19	13	68.4	46	35	76.1
OA	27	6	22.2	20	4	20.0	47	10	21.3
Non-specific infection									
Sub-periosteal new bone	40	24	60.0	23	19	82.6	63	43	68.3

Sinusitis	38	7	18.4	12	1	8.3	50	8	16.0
Specific infection	40	2	5.0	23	2	8.7	63	4	6.3
Circulatory	30	8	26.7	22	9	40.9	52	17	32.7
Metabolic									
Cribra orbitalia	38	9	23.7	21	7	33.3	59	16	27.1
Scurvy/Rickets	13	1	7.7 (of non-adults)	4	0	0	17	1	5.9 (of non-adults)
Neoplastic	40	9*	22.5	23	3*	13.0	63	11*	17.5

APPENDIX 3: Skeleton Catalogue (in separate PDF)